We thank all the reviewers (including the editor) for their useful suggestions and insight. We have made appropriate changes in our manuscript to incorporate the reviewer comments. Based on verbal conversations with experts in the field, we have also made a small change to the title replacing "primary organic aerosol" with "freshly emitted organic aerosol" as we are not certain that no secondary processes occur within the volume of our chamber leading to sampling of some secondary aerosols as well. Below are our responses to concerns brought up by the reviewers with reviewer comments in **boldface** followed by our reply.

Review:

Dr. Sergey Nizkorodov

Dear authors. As reviewers pointed out, the revised version has improved considerably. Please address the remaining points raised by reviewers #1 and #2 of the revised manuscript. In addition, I have a few editorial review notes below, which may also need to be addressed before the final acceptance.

Line 157: a space is needed between l and min

The space has been added

Line 170: there is another important artifact of changing the chemical composition by sonochemistry, as described in [Mutzel, A.; Rodigast, M.; Iinuma, Y.; Böge, O.; Herrmann, H., An improved method for the quantification of SOA bound peroxides. Atmos. Environ. 2013, 67, (0), 365-369.] You might want to cite it.

The citation has been added along with the line: "…and to avoid changes in chemical composition caused by acoustic cavitation (Mutzel et al., 2012)". Thank you for providing this citation.

Line 173: impurities -> suspended particles (because filtration does not remove soluble impurities)

Impurities has been changed to suspended particles

Line 182: this effectively sets the absorption coefficient at 700 nm to zero. Please discuss in the paper whether it was actually the case for your samples (in many cases absorbance at 700 nm is indeed negligible). It might be more precise to subtract an average absorbance over a wavelength interval where you expect no absorption, such as 700-750 nm as opposed to subtracting a single value, which is prone to more uncertainty. I do not suggest you should redo all of your calculations, just a suggestion for the future.

We now mention that the absorbance at 700 nm was negligible and close to zero for our samples. The value of 700 nm was selected based on the convention set by previous studies. However, we

agree that an average value over the long wavelength range would be more appropriate for future calculations. The authors thank you for the suggestion.

Line 189: please fix grammar in this sentence

The sentence now reads: “It was assumed that all the absorption at 1047 nm could be attributed to BC aerosol (Bahadur et al., 2012)”

Line 235: I think conversion of WSOC into mass concentration of dissolved organics requires an OM/OC ratio. What was the assumed value?

The mass concentrations mentioned here are OC mass concentrations. The sentence now reads: “In the given study, the OC mass concentration was measured…” to get rid of any confusion. We have also added a line stating that the obtained refractive index is representative of OC and not OM: “It is important to note that k values obtained using this method will represent optical characteristics of OC mass and not total organic mass.”

Table 4: there are too many significant digits reported in AAE values. There is no reason to report uncertainties with more than 1-2 significant digits. The entry 13.74+/-2.27 would be more faithfully represented as 14+/-2 or 2 13.7+/-2.3. Similar considerations apply to numbers reported in a few other tables as well as text.

The number of significant figures has been reduced for AAE and fit coefficients. These have been modified throughout the text as well.

Several references have an incomplete list of authors, for example, Akagi et al. (2011), Arnott et al. (2003). I think your reference manager software is cutting the list. ACP lists all authors to the best of my knowledge, so it needs to be fixed.

Also, fix page numbers in references Arnott et al. (2003), Bahadur et al. (2012), Kirchstetter et al. (2004), Saleh et al. (2015), Sun et la. (2007), Zhang et al. (2008). I am guessing your reference library is missing these page numbers and formatting the references incorrectly. It is a common problem form AGU journals.

Panteliadis et l. (2015) reference is missing the journal

All the references have been fixed according to the ACP standard, thank you for pointing these out.

Anonymous Referee #2:

Shetty et al's new version of the manuscript is much clearer and addressed the major concerns highlighted in the reviewer comments. However, I still see some minor errors and contents that need to be addressed in the manuscript.

In the manuscript, the symbols in each equation and in the text should be written in the same format such as in the Microsoft Equation format. It seems that, in the text, symbols are written in Microsoft font and not in the Microsoft equation format.

The symbols have been modified to the Microsoft equation format in both the text as well as in equations

I recommend using a comma between two lambdas (in line 196: λ1, λ2).

The "and" was replaced with a comma.

In page 319, add a line by giving a reference that can be referred to obtain 0.39 for BC using parametrization at OC/TC ratio of 0 (Line 319) or add a line to support it. Also, explain is it possible to observe OC/TC as zero (line 319)?

We have added references stating that observations from most studies give lower SSA, but those by Radney et al. (2014) are closer to values obtained from our parametrizations. The line reads: "Most observations for soot SSA are lower than those predicted by our 405 nm parametrizations (Bond et al., 2013, Schnaiter at al., 2003) with our projections being closer to SSA observed by Radney et al. (2014)."

We have also changed the sentence from OC/TC of 0 to: "…SSA value of 0.39 for pure EC obtained using our parametrization." bypassing the need for explaining observations having OC/TC ratios of zero.

In lines 353-354, Fig. 5 does not tell anything about EC fractions>0.25 and typical BB as stated in the text. Add a line showing how it is associated with Fig. 5.

EC fractions > 0.25 are representative of values with OC/TC ratios < 0.75 as depicted in Fig. 5. We have changed "EC fractions > 0.25" to "EC/TC ratios > 0.25". While Fig. 5 does not say anything about typical BB, the previous line references typical OC/TC values observed for lab- and field-based BB experiments justifying the need to exclude these points from our analysis.

Section 3.4, the title is recommended to rewrite such as Scaling Factors Based on Mie calculations.

The title of Section 3.4 was changed.

In line 408-409, it seems ambiguity of suggesting researchers avoid such scaling factors for determining OA absorption without exact knowledge of OC extraction efficiencies and particle size distributions. I suggest to authors to present data or references to support how knowledge of OC extraction efficiencies and particle size distributions will convince of using scaling factors for determining OA absorption.

We thank the reviewer for pointing out the apparent ambiguity in the sentence. We have changed the sentence to "We recommend future studies to use caution and judgement when using *a priori* scaling factors for determining OA absorption using solvent extraction techniques."

Anonymous Referee #5:

1) The trends in Figure 2 and Figure 5 seem to be unrealistic, or at least inconsistent with the argument (Line 358-365) that extraction efficiency increases with increasing OC/TC (and thus, SSA). Specifically, in panel (b), how do the authors explain the sharp drop in babs,OA/babs,sol to values close to zero at high OC/TC and SSA? One would expect babs,OA/babs,sol to approach a constant value (due only to particle size effects) with increasing extraction efficiency, so one should expect an asymptotic behavior of babs,OA/babs,sol at large OC/TC and SSA values, opposite to what's observed. It seems to me that the observed trends could be partially an artifact of the way babs,OA is calculated as the difference between the measured babs,tot and a calculated babs,BC (section 2.2.2). In any case, a discussion of the meaning of the trends observed at large SSA values should be added to section 3.1.

The argument for decreasing extraction efficiencies in water was used to explain the increasing difference in absorption bias between water and methanol extracts. In panel (b) for methanol and acetone extracts, rather than being close to zero, these values were close to 0.6 for some dung samples which are similar to theoretical predictions by Sun et al. (2007) for particles much smaller than the wavelength of light; but we were not confident of justifying these observations based on this argument as our size distributions were comparable to the light wavelength of 405 nm. We have added a line to acknowledge these observations in Section 3.1.

Based on our observations, we believe that the extraction efficiency would not decrease indefinitely but tend towards a constant value above a given EC/OC fraction depending on the type of organics released, mimicking an exponential function comparable to observed trends in biomass burning OA wavelength dependence with EC/OC ratios (Saleh et al., 2014) and OA refractive indices (Saleh et al., 2018). This would lead to the bias approaching a constant value (due only to particle size effects) with decreasing OC/TC ratios and in turn the aerosol SSA. The text in the revised manuscript has been modified to better reflect this fact. The authors thank the reviewer for pointing the ambiguity in our explanation.

Based on sound absorption theories, we do not believe that our observations are an artifact of the calculations. For example, the widely accepted band-gap model (Moosmüller et al., 2011) has been used to support a BC AÅE of 1; this value has been used by the community to extrapolate spectral absorption coefficients from longer to shorter wavelengths across the near-UV-Vis-NIR solar spectrum. The ideal nature of the band gap model could have deviations, leading to observed BC AÅE ranging from 0.85 to 1.1 as found in other studies (Lack et al., 2008; Bergstrom et al., 2007; Lan et al., 2013), and these extremes have been taken into consideration in our study for sensitivity calculations.

2) Along the same lines, the data, especially the part of the space that has the sharp change (i.e. SSA > 0.9), should be further explored. For example, the data in Figure 2 could be plotted with the points color-coded by fuel type and with different scales on the y-axis to better zoom in the changes at SSA > 0.9 to see if the variability that is not explained by SSA

(i.e. where the changes are very steep) could be explained by fuel type. The same applies to OC/TC.

The authors could not find any variability that could be clearly explained by the fuel type, and no interesting or noticeable findings were observed with exploring the data near the sharp change. Color coding the points based on fuel type was a helpful suggestion, however doing so made the figures busy and hard to follow. We have incorporated the reviewer's suggestion by modifying the figures with different markers for each fuel and color coded based on the solvent used for extraction. As the effects of fuel type were not apparent, these have not been discussed in the manuscript.

3) Line 275 – 281: the choice of SSA = 0.7 and 0.825 as a cutoff between low uncertainty and high uncertainty ranges seems arbitrary. What constitutes high uncertainty? Also, in Figure 2, similar size error bars (especially in panel b) seems to exist on both sides of the cutoff lines.

While the error bars were calculated using the Monte Carlo simulations, the cutoff for high and low uncertainty was based on sensitivity to range of BC AÅE observed by past researchers. For samples below the cutoff, a change in BC AÅE from 0.8 to 1.1 led to drastic changes in the $b_{abs,OA}/b_{abs,sol}$ values with uncertainties greater than 30%, and in one case exceeding 200%. The high uncertainties were a direct result of the high absorption coefficient at 1047 nm for the given samples. We have modified the text to indicate what constitutes high uncertainty in our analysis. As the error bars were calculated with the Monte-Carlo simulations, the errors seem to be similar on both sides of the cutoff line, but the points above the cutoff have slightly smaller sensitivity to BC AÅE than the points below it.

4) The purpose and value of the Mie calculations in section 3.4 are not clear. It reads: previous studies have used scaling factors of 2. This study found a scaling factor of 2. In conclusion, a scaling factor of 2 should not be used because of reasons stated in the previous sections. Then why do the Mie calculations to begin with? The cautionary statement about the non-universality of the scaling factor of 2 should be inserted in section 3.1.

The presentation of the results could be reformulated in a more informative way. For the 3 experiments reported in section 3.2, the authors can compare babs,OA, babs,sol, and babs,Mie and use this comparison to determine the fractional contribution of particle size and extraction efficiency to the discrepancy.

The Mie calculations were added to check the reproducibility of the conventionally used scaling factor. We found that the factor was reproducible for the samples that we tested; however, these values had errors while predicting particle phase absorption coefficients and pointing this out through our calculations was the purpose of this section. We have modified the text in this section to explain this better.

The extraction efficiency for the tested samples were close, with 61 ± 2% extraction of organics for the three samples. As the actual differences in the scaling factors is not significant, and the Mie Calculations were not too sensitive to the particle size distributions we did not find it helpful to compare $b_{abs,OA}$, $b_{abs,sol}$ and $b_{abs,Mie}$ separately. We have however modified the text to better explain the reason for this section

5) Table 4: It would be more informative to present the data in Table 4 as scatter plot of AAE_OA vs AAE_sol, color coded with fuel type and with a 1:1 line.

We tried depicting the data using a scatter plot along with error bars, but the final plots looked very busy and did not provide better insights than those obtained using the Table along with a t-test analysis. For this reason, we preferred to represent the data using the table rather than a scatter plot. We however thank the reviewer for their suggestion and have added a similar plot in the supplementary section representing particle phase AAE and AAE data from each solvent extract, having different markers based on fuel type.

6) Table 5: with geometric mean diameter of 397 nm, the size distribution is expected to extend beyond the SMPS measurement window. It is not clear how this issue was addressed.

The issue was resolved by extending the SMPS data using the equation for a lognormal function. A line has been added to the methods section 2.3 clarifying the same: "If size distributions extended over the SMPS measurement range, the data were extrapolated using a lognormal equation."

References:

Bergstrom, R. W., Pilewskie, P., Russell, P. B., Redemann, J., Bond, T. C., Quinn, P. K., and Sierau, B.: Spectral absorption properties of atmospheric aerosols, Atmos. Chem. Phys., 7, 5937-5943, https://doi.org/10.5194/acp-7-5937-2007, 2007.

Bond, T. C., Doherty, S. J., Fahey, D., Forster, P., Berntsen, T., DeAngelo, B., Flanner, M., Ghan, S., Kärcher, B., and Koch, D.: Bounding the role of black carbon in the climate system: A scientific assessment, J. Geophys. Res-Atmos., 118, 5380-5552 , https://doi:10.1002/jgrd.50171, 2013.

Lack, D. A., Cappa, C. D., Covert, D. S., Baynard, T., Massoli, P., Sierau, B., Bates, T. S., Quinn, P. K., Lovejoy, E. R., and Ravishankara, A.: Bias in filter-based aerosol light absorption measurements due to organic aerosol loading: Evidence from ambient measurements, Aerosol Sci. Tech., 42, 1033-1041, https://doi.org/10.1080/02786820802389277, 2008.

Lan, Z.-J., Huang, X.-F., Yu, K.-Y., Sun, T.-L., Zeng, L.-W., and Hu, M.: Light absorption of black carbon aerosol and its enhancement by mixing state in an urban atmosphere in South China, Atmos. Environ., 69, 118-123, https://doi.org/10.1016/j.atmosenv.2012.12.009, 2013.

Moosmüller, H., Chakrabarty, R., Ehlers, K., and Arnott, W.: Absorption Ångström coefficient, brown carbon, and aerosols: basic concepts, bulk matter, and spherical particles, Atmos. Chem. Phys., 11, 1217-1225, https://doi.org/10.5194/acp-11-1217-2011, 2011.

Radney, J. G., You, R., Ma, X., Conny, J. M., Zachariah, M. R., Hodges, J. T., and Zangmeister, C. D.: Dependence of soot optical properties on particle morphology: measurements and model comparisons, Environ. Sci. Technol., 48, 3169-3176, https://doi.org/10.1021/es4041804, 2014.

Schnaiter, M., Horvath, H., Möhler, O., Naumann, K.-H., Saathoff, H., and Schöck, O.: UV-VIS-NIR spectral optical properties of soot and soot-containing aerosols, J. Aerosol Sci., 34, 1421-1444, https://doi.org/10.1016/S0021-8502(03)00361-6, 2003.

Saleh, R., Robinson, E. S., Tkacik, D. S., Ahern, A. T., Liu, S., Aiken, A. C., Sullivan, R. C., Presto, A. A., Dubey, M. K., and Yokelson, R. J.: Brownness of organics in aerosols from biomass burning linked to their black carbon content, Nat. Geosci., 7, 647–650, https://doi.org/10.1038/ngeo2220, 2014.

Saleh, R., Cheng, Z., and Atwi, K.: The brown–black continuum of light-absorbing combustion aerosols, Environ. Sci. Tech. Let., 5, 508-513, 2018.

Sun, H., Biedermann, L., and Bond, T. C.: Color of brown carbon: A model for ultraviolet and visible light absorption by organic carbon aerosol, Geophys. Res. Lett., 34, L17813, https://doi.org/10.1029/2007GL029797, 2007.

Measuring Light Absorption by ~~Primary~~ Freshly Emitted Organic Aerosols: Optical Artifacts in Traditional Solvent Extraction-Based Methods

Nishit J Shetty[1], Apoorva Pandey[1], Stephen Baker[2], Wei Min Hao[2], Rajan K. Chakrabarty[1,3]

[1]Center for Aerosol Science and Engineering, Department of Energy, Environmental and Chemical Engineering, Washington University in St. Louis, St. Louis, MO 63130, USA

[2]USDA Forest Service, Rocky Mountain Research Station, Fire Sciences Laboratory, Missoula, Montana, USA

[3]McDonnell Center for the Space Sciences, Washington University in St. Louis, St. Louis, MO 63130, USA

Correspondence to: Rajan K. Chakrabarty (chakrabarty@wustl.edu)

Abstract

Recent studies have shown that organic aerosol (OA) could have a non-trivial role in atmospheric light absorption at shorter visible wavelengths. Good estimates of OA absorption are therefore necessary to accurately calculate radiative forcing due to these aerosols in climate models. One of the common techniques used to measure OA light absorption is the solvent extraction technique from filter samples which involves the use of a spectrophotometer to measure bulk absorbance by the solvent-soluble organic fraction of particulate matter. Measured solvent phase absorbance is subsequently converted to particle-phase absorption coefficient using scaling factors. The conventional view is to apply a correction factor of 2 to absorption coefficients obtained from solvent-extracted OA based on Mie calculations. The appropriate scaling factors are a function of biases due to incomplete extraction of OC by solvents and size-dependent absorption properties of OA. The range for these biases along with their potential dependence on burn conditions is an unexplored area of research.

Here, we performed a comprehensive laboratory study involving three solvents (water, methanol, and acetone) to investigate the bias in absorption coefficients obtained from ~~the~~ solvent extraction-based photometry techniques as compared to in-situ particle phase absorption for ~~primary~~ freshly emitted OA ~~emitted~~ from biomass burning. We correlated the bias with OC/TC mass ratio and single scattering albedo (SSA) and observed that the conventionally used correction factor of 2 for water and methanol-extracted OA might not be extensible to all systems and suggest caution while using such correction factors to estimate particle-phase OA absorption coefficients. Furthermore, a linear correlation between SSA and OC/TC ratio was also established. Finally, from the spectroscopic data, we analyzed the differences in Absorption Ångström Exponents ($\AA E$~~AÅE~~) obtained from solution- and particulate-phase measurements. We noted that $\AA E$~~AÅE~~ from solvent phase measurements could deviate significantly from their OA counterparts.

1 Introduction

Carbonaceous aerosols constitute a major short-lived climate pollutant, and even though they have been studied extensively in recent years, estimates of their contribution to shortwave radiative forcing remains highly uncertain (IPCC, 2013). Based on their thermal-refractory properties, carbonaceous aerosols are categorized as elemental carbon (EC) or organic carbon (OC) (Chow et al., 2007b; Bond et al., 2013), and the sum of OC and EC is referred to as total carbon (TC). When defined optically, the refractory EC component is approximately referred to as black carbon (BC) (Chow et al., 2007b; Bond et al., 2013); BC aerosol constitute the strongest of the light absorbing aerosol components in the atmosphere (Ramanathan and Carmichael, 2008; Andreae and Gelencsér, 2006; IPCC, 2013). While BC absorbs strongly in the visible spectrum, the contribution of OC towards absorption has largely been neglected, even though many studies have demonstrated significant OC absorption at lower visible wavelengths (Yang et al., 2009; Chen and

Bond, 2010; Chakrabarty et al., 2010; Kirchstetter 2012). The atmospheric mass of OC can be 3-12 times larger than that of BC (Husain et al., 2007; Zhang et al., 2008) which warrants its inclusion as an atmospheric light absorber. Only recently have global modeling studies started incorporating radiative forcing by organic aerosol (OA) absorption (Wang et al., 2014; Saleh et al., 2015; Lin et al., 2014; Wang et al., 2018). Thus, having accurate estimates for OA absorption is necessary to help improve climate models.

A convenient and prevalent methodology of measuring OA absorption is based on collecting aerosol particles on a filter substrate followed by extracting the organic compounds into a solvent. This analytical method is used in many studies as it ideally excludes any interference from EC and primarily provides the absorption spectra of extracted OC (Mo et al., 2017; Chen and Bond, 2010; Liu et al., 2013). The absorbance of organic chromophores in the solvent extract is measured using an ultraviolet-visible (UV-Vis) spectrophotometer and measured absorbance values can be converted to corresponding solvent phase absorption coefficients ($b_{abs,sol}$ ~~$b_{abs,sol}$~~). However, this methodology has limitations as it is unable to represent size-dependent absorption properties of the extracted OA (Liu et al., 2013; Washenfelder at al., 2015; Moosmüller et al., 2011). To correct for this limitation, the complex refractive index (RI) of OC is estimated by assuming the real part and calculating the imaginary part for extracted OC using $b_{abs,sol}$ ~~$b_{abs,sol}$~~ and dissolved OC concentration, the complex RI is then used along with a number size distribution as inputs to Mie theory for calculating the particle-phase absorption coefficient for dissolved OC. In addition to discrepancies between particle and solvent phase optical properties, the method suffers from biases due to incomplete extraction of organics by different solvents (Chen and Bond, 2010; Liu et al., 2013) which lead to differences in values of $b_{abs,sol}$ ~~$b_{abs,sol}$~~ obtained from different solvents. The significance and extent of this bias varies based on the OC extraction efficiency of a given solvent

and would be negligible for solvents extracting 100% of organic chromophores. A combination of inefficient organic carbon extraction and the methods inability to measure size-dependent OA absorption properties can result in significant errors to optical properties obtained using this method. Despite the low OC extraction efficiency of water (Chen and Bond, 2010) and large potential for errors, past studies have used light absorption by water soluble organic carbon (WSOC) as a surrogate for OA optical properties (Bosch et al., 2014; Kirillova et al., 2014a; Kirillova et al., 2014b). However, the use of water as an OA surrogate is decreasing with more recent studies using methanol to extract OC (Cheng et al., 2016; Shen at al., 2017; Xie et al., 2017). While methanol has a higher OC extraction efficiency than water (Chen and Bond, 2010), its efficiency is limited ranging from 85-98% (Cheng et al., 2016; Xie et al., 2017) which can lead to misrepresentation of OA optical properties if the unextracted fraction correspond to extremely low volatility organic carbon (ELVOCs) or similar organic chromophores which have large light absorption efficiencies (Saleh et al., 2014), underscoring the need for a more complete extraction protocol. In addition to problems with incomplete OC extraction, previous studies have attempted to correct for size-dependent biases using absorption coefficients determined with Mie theory and provided a narrow range of solvent-dependent scaling factors from 2 for water extracts to 1.8 for methanol extracts, all corresponding to a mean particle diameter of 0.5 μm (Liu et al., 2013; Liu et al., 2016; Washenfelder et al., 2015). Sun et al. (2007) performed theoretical calculations and postulated a correction range of 0.69 - 0.75 for OC particles with diameters much smaller than the wavelength of light. These correction factors while applicable to these individual systems, might not be extensible to aerosol emissions from other combustion events. However, many studies have used scaling factors from such studies on absorption coefficients obtained from solvent phase optical measurements despite potential differences in system dependent biases for each experiment

(Kim et al., 2016; Zhang et al., 2017; Wang et al., 2018). To the authors knowledge, no attempts have been made to explicitly study or quantify these biases with varying aerosol intrinsic properties, such as the EC/OC ratios, and single scattering albedo (SSA), even though these properties have shown to be well correlated with OA optical properties (Zhang et al., 2013; Saleh at al., 2014; Bergstrom et al., 2007).

In-situ measurement of particulate-phase absorption coefficient is commonly and accurately accomplished using a photoacoustic spectrometer (PAS) (Lack et al., 2006; Arnott et al., 2005; Arnott et al., 2003). However, on its own, a single-wavelength PAS cannot distinguish between absorption by OC and BC aerosol and it typically measures the total particle-phase absorption coefficient ($b_{abs,tot}$ ~~$b_{abs,tot}$~~) of the aerosol population in the cell (Moosmüller et al., 2009). One can make use of a multi-wavelength PAS using which the OA absorption coefficient ($b_{abs,OA}$ ~~$b_{abs,OA}$~~) could be separated out from that of BC absorption, based on the difference in BC and OA Absorption Ångström Exponent (*AÅE* ~~*AÅE*~~) (Washenfelder et al., 2015; Arola et al., 2011; Kirchstetter and Thatcher; 2012). The *AÅE* ~~*AÅE*~~ for pure BC is well-constrained at 1 in the visible and near-infrared wavelengths (Moosmüller et al., 2009). The value of $b_{abs,OA}$ ~~$b_{abs,OA}$~~ is calculated as the difference between $b_{abs,tot}$ ~~$b_{abs,tot}$~~ and the BC absorption coefficient. A possible technique to measure the bias between particle and solvent phase organic absorption ($b_{abs,OA}$/ $b_{abs,sol}$ ~~$b_{abs,OA}$/$b_{abs,sol}$~~) can thus be established by carrying out simultaneous measurements of solution- and particle-phase absorption properties during a study. Determining $b_{abs,OA}$ ~~$b_{abs,OA}$~~ using this method gives large errors when BC absorption coefficient is large or comparable to $b_{abs,tot}$ ~~$b_{abs,tot}$~~ as $b_{abs,OA}$ ~~$b_{abs,OA}$~~ would be a small number obtained by the subtraction of two large numbers limiting the use of this technique for relatively low EC/OC ratios.

Here, we burnt a range of different biomass fuels under different combustion conditions and the resulting aerosol emissions were passed through various in-situ instruments while simultaneously being collected on quartz-fiber filters. The particle phase absorption coefficient was obtained using integrated photoacoustic-nephelometer spectrometers (IPNs) at wavelengths 375, 405 and 1047 nm. Organics collected on quartz-fiber filters were extracted in water, acetone, and methanol, and corresponding $b_{abs,sol}$ ~~$b_{abs,sol}$~~ values were calculated. These values were compared with corresponding $b_{abs,OA}$ ~~$b_{abs,OA}$~~, and the change in $b_{abs,OA}/b_{abs,sol}$ ~~$b_{abs,OA}/b_{abs,sol}$~~ with varying single scattering albedo (SSA) values and OC/TC ratios was examined. SSA was parametrized with the OC/TC ratios with trends similar to those observed by Pokhrel et al.~~,~~ (2016). $\text{Å}E$ ~~$\text{Å}E$~~ from spectroscopic data for solution and particle phase measurements were compared, and the Mie Theory based correction factor was also investigated for a few samples.

2 Methods:

2.1 Sample generation and collection

Fig. 1 is a schematic diagram of our experimental setup, which consist~~s~~ed of a sealed 21 m^3 stainless-steel combustion chamber housing a fan for mixing and recirculation (Sumlin et al., 2018b). Aerosol samples were generated by burning several types of biomass including pine, fir, grass, sage, and cattle dung (details are provided in the Supplementary Information). During a chamber burn, 10-50 g of a given biomass was placed in a stainless-steel pan and ignited by a butane lighter. The chamber exhaust was kept closed for the duration of a given experiment. The biomass bed was either allowed to burn to completion or it was prematurely extinguished and brought to a smoldering phase by extinguishing the flame beneath a lid. Different combustion

conditions were used to generate samples with varying properties: OC/TC ratios ranged from 0.55-1, and SSA values ranged from 0.56-0.98 for wavelengths of 375, 405, and 1047 nm.

For one set of experiments, the particles were directly sampled from the chamber; in another set, the sampling was done from a hood placed over the burning biomass. A diffusion dryer removed excess water from the sample stream, and the gas-phase organics were removed by a pair of activated parallel-plate semi-volatile organic carbon (SVOC) denuders. The gas-phase organics were stripped to reduce artifacts produced by the adsorption of organic vapors on the quartz filters. The aerosols were finally sent to a 208-liter stainless-steel barrel, from which they were continuously sampled by the three IPNs. Some phase repartitioning of condensed SVOC into the vapor phase may take place post the denuders in our holding tank and would introduce a positive bias to our filter-based measurements. The experiments were conducted in two sets, the first set included a scanning mobility particle sizer (SMPS, TSI, Inc.) and size measurements from this instrument were used in Mie Theory calculations detailed in Section 2.3. The SMPS was not used in the second set of experiments due to problems with aerosol flows in the system. However, the SMPS data from the first set of experiments gave us an estimate of the range over which the size distributions varied and was used to obtain the geometric mean of the size distribution. The real-time absorption and scattering coefficients were measured by the IPNs, and samples were simultaneously collected on quartz fiber filters once a steady state signal was achieved. The absorption and scattering coefficients were used to calculate the SSA, which is simply the scattering coefficient divided by the extinction coefficient. Radiative forcing calculations for absorbing OC require good estimates of OC absorption at different SSA values (Lin et al, 2014; Feng et al, 2013; Chakrabarty et al, 2010) underscoring the need to study OA absorption biases as a function of SSA. The particles were passed through the filter samplers at a flowrate of 5 L min^{-1}

[1], with sampling times ranging from 2-15 minutes. Two or more filters were collected for a given steady state condition. One of these filters was used to determine the OC and EC fractions of the deposited particles, and the other filters were used for the extraction experiments. The only exception to this case is one sample of emissions from dung combustion where the resultant aerosol was assumed to be purely organic based on a purely smoldering combustion phase and by comparing with optical properties from previous experiments.

2.2 Analytical t~~T~~echniques

2.2.1 Absorption by solvent extracted OC

Quartz filters (Pallflex Tissuquartz, 47 mm diameter) collected during sampling were split into four quarters, and each quarter was extracted using either deionized water, acetone, hexane, or methanol. The absorption by hexane extracts were low and prone to errors, so data for its extracts were not analyzed. The filters were placed in 3-5 ml of the solvent for 24 hours. The filter was not sonicated to reduce artifacts from mechanical dislodging of BC particles (Phillips and Smith, 2017) and to avoid changes in chemical composition caused by acoustic cavitation (Mutzel et al., 2012). The solvent volumes were measured both before and after the extraction and the differences between the two measurements were within 8%. The extracts were then passed through syringe filters with 0.22 μm pores to remove any ~~impurities~~ suspended particles introduced ~~by~~ during the extraction process.

The light absorbance of the extracts was measured using a UV-Vis spectrophotometer (Varian Inc., Cary 50) at wavelengths from 300 nm to 800 nm. To compare the absorbance ($A(\lambda)$)~~(A(λ))~~ of chromophores in the solution with the absorption coefficient of the particles in the atmosphere,

all absorbance values were converted to solution-phase absorption coefficients at given wavelengths ($b_{abs,sol}(\lambda)$ ~~$b_{abs,sol}(\lambda)$~~) (Liu et al., 2013):

$$b_{abs,sol}(\lambda) = (A(\lambda) - A(700))\frac{V_l}{V_a * l}\,.\ln(10), \quad (1)$$

where V_l ~~V_l~~ is the volume of solvent the filter was extracted into, V_a ~~V_a~~ is the volume of air ~~that~~ passed over the given filter area, and l ~~l~~ is the optical path length that the beam traveled through the cuvette (1 cm). ~~The a~~Absorbance at a given wavelength is normalized to ~~the~~ absorbance at 700 nm to account for any signal drift within the instrument. Absorbance at 700 nm was negligible and close to zero for the analyzed samples indicating no absorption at long wavelengths and little to no signal drift for the instrument. The resulting absorption coefficient (m^{-1}) was multiplied by ln(10) to convert from log base 10 (provided by the UV-Vis spectrophotometer) to natural log.

2.2.2 Absorption by BC and OC in particle phase

To estimate the BC absorption at 375 nm and 405 nm, the absorption data from the IPN operated in the infrared regime at a wavelength of 1047 nm was converted to equivalent BC particulate absorption at the near UV wavelengths, using a BC absorption Ångström exponent ($AÅE_{BC}$ ~~$AÅE_{BC}$~~) value of 1 (Kirchstetter et al., 2004; Andreae and Gelencsér, 2006). ~~The assumption here being~~It was assumed that all the absorption at 1047 nm could be attributed to BC aerosol (Bahadur et al., 2012). The BC light absorption coefficient at shorter wavelengths ($b_{abs,BC}(\lambda)$ ~~$b_{abs,BC}(\lambda_1)$~~) was calculated by:

$$b_{abs,BC}(\lambda_1) = b_{abs,tot}(1047).\left(\frac{\lambda_1}{1047}\right)^{-AÅE_{BC}}, \quad (2)$$

where λ_1 is the wavelength at which the absorption will be calculated and $\text{Å}AE$ ~~$AÅE$~~ is defined for a pair of wavelengths λ_1, ~~and~~ λ_2 as the exponent in a power law expressing the ratio of the absorption coefficients as follows (Moosmüller et al., 2009):

$$\text{Å}AE(\lambda_1\lambda_2) = \frac{ln\left[{b_{abs}(\lambda_1)}/{b_{abs}(\lambda_2)}\right]}{ln\left[{\lambda_2}/{\lambda_1}\right]} \quad (3)$$

$\text{Å}AE$ ~~$AÅE$~~ is an optical descriptor of the inherent material property. For BC particles, typical values of $\text{Å}AE$ ~~$AÅE$~~ ≈1, while for OC particles $\text{Å}AE$ ~~$AÅE$~~ > 4 (Moosmüller et al., 2009). The value of $b_{abs,BC}$ ~~$b_{abs,BC}$~~ at 375nm and 405nm was then subtracted from $b_{abs,tot}$ ~~$b_{abs,tot}$~~ at those wavelengths to calculate $b_{abs,OA}$ ~~$b_{abs,OA}$~~. The ratio $b_{abs,OA}/b_{abs,sol}$ ~~$babs,OA(\lambda)/babs,sol(\lambda)$~~ was calculated to represent the scaling bias between the bulk solvent phase absorption coefficient and OA absorption coefficient.

The organic and elemental carbon compositions of the filters were measured with a thermal-optical OC/EC analyzer (Sunset Laboratory, Tigard, OR) using the Interagency Monitoring of Protected Visual Environments (IMPROVE)-A Thermal/Optical Reflectance (TOR) analysis method (Chow et al., 2007a). The OC/TC ratios were assumed to be constant for a given steady state IPN reading, which allowed us to relate the absorption data to the OC/TC data. The assumption was tested by performing EC/OC analysis of two filters collected during a given steady state for a burn. The OC/TC ratio remained unchanged or within experimental error for the burns and results for the EC/OC analysis of tested filters are provided in Table S1 and S2 of the Supplementary Information.

2.2.3 Uncertainty using Monte Carlo simulations

The uncertainties due to error propagation were evaluated using a Monte Carlo approach. The true measurement value was assumed to possess a Gaussian probability distribution with mean and

standard deviation values corresponding to measured values and instrument specifications respectively. Calculations were performed by randomly selecting values based on the probability distribution for the different variables and corresponding values for $b_{abs,OA}/b_{abs,sol}$ ~~$b_{abs,OA}/b_{abs,sol}$~~ were estimated. A total of N = 10000 iterations w~~as~~ere performed for each data point and each simulation was rerun 100 times till the $b_{abs,OA}/b_{abs,sol}$ ~~$b_{abs,OA}/b_{abs,sol}$~~ value converged for the calculations. The propagated error~~–~~ due to ~~the~~ uncertainty in important ~~all~~ variables was then calculated as the standard deviation of $b_{abs,OA}/b_{abs,sol}$ ~~$b_{abs,OA}/b_{abs,sol}$~~ values ~~obtained~~ acquired over ~~all the~~ simulations. A pseudocode for the Monte Carlo ~~simulation~~ calculation is detailed in the Supplementary Information along with Table S~~3~~4 which denotes typical mean and standard deviation values used for variables with uncertainties.

2.3 Mie t~~T~~heory ~~C~~calculations

A commonly used method to correct for differences between the chromophore absorption in solution and aerosol particle absorption is by using Mie Theory (Liu et al., 2013; Washenfelder et al., 2015). The imaginary part (k) of the complex refractive index $m = n + ik$ can be determined from bulk solution phase absorption data and converted to equivalent OA absorption using Mie Theory along with assumptions regarding the shape of the particles and the real part of the ~~particles~~ complex refractive index of the particle.

To find k, the mass absorption efficiency (α/ρ) ~~α/ρ~~ was determined using the absorbance data and the OC mass concentration in the solution (Liu et al., 2013):

$$\frac{\alpha(\lambda)}{\rho} = \frac{b_{abs,sol}(\lambda)}{M}, \quad (4)$$

where $b_{abs,sol}(\lambda)$ ~~$b_{abs,sol}(\lambda)$~~ is the solvent-phase absorption coefficient determined in Eq. (1), and M is the mass concentration of OC in the solution. In the given study, the OC mass concentration was measured for some of the water extracts using a total organic carbon (TOC) analyzer (Shimadzu, TOC-L). The ~~corresponding~~ water-soluble organic carbon (WSOC) was then used to estimate α/ρ ~~α/ρ~~ of the solution. The calculated α/ρ ~~α/ρ~~ was further used to determine k for the WSOC by (Chen and Bond 2010):

$$k(\lambda) = \frac{\rho.\lambda.\left(\frac{\alpha(\lambda)}{\rho}\right)}{4\pi}, \quad (5)$$

where λ is the light wavelength at which k needs to be calculated, and ρ is the density of the dissolved organic compounds. A ρ value of 1.6 (Alexander et al., 2008) was used to calculate the k values, and was also used in all subsequent calculations using density. It is important to note that k values obtained using this method will represent optical characteristics of OC mass and not total organic mass. A Mie based inversion algorithm was used to extract the real part of the refractive index (n) using data from the SMPS and IPN (Sumlin et al., 2018a). If size distributions extended over the SMPS measurement range, the data w~~as~~ere extrapolated using a lognormal equation. A sensitivity analysis was performed by varying the n value from 1.4 to 2, and the change in Mie calculated absorption was within 18%. The size distribution for the WSOC was estimated assuming the same geometric mean and standard deviation as that of the original aerosol, but with number concentrations calculated based on the extracted mass. Calculations for the number concentration are provided in the Supplementary Information. After the size distribution and complex refractive index were determined, they were used to calculate the absorption coefficient based on Mie Theory, which was then compared to $b_{abs,sol}$ ~~$b_{abs,sol}$~~ to verify the traditional Mie based scaling factors for converting from solution to particle phase absorption.

3 Results and discussion

3.1 Absorption bias correlated with ~~S~~single ~~s~~Scattering ~~a~~Albedo

Fig. 2 shows the trends in $b_{abs,OA}/b_{abs,sol}$ ~~$b_{abs,OA}(\lambda)/b_{abs,sol}(\lambda)$~~ for ~~primary~~ fresh organic aerosol emissions with varying SSA. The different fuel types are marked with distinct markers and ~~T~~the error bars are estimated from the results of the Monte Carlo simulation and account for uncertainties in IPN measurements, UV-Vis spectrophotometer measurements, filter sampling flowrates, BC ~~*AÅE*~~ *AÅE* based uncertainties and extract volume measurements. Measured SSA for pure fractal BC aggregates have values between 0.1-0.~~4~~3 (Schnaiter et al., 2003; Bond et al., 2013) depending on the size of the BC monomers (Sorensen 2001), and due to this particularly low SSA of BC compared to OC, an increase in ~~the~~ BC content of ~~the~~ aerosol composition would lead to decreasing SSA. This relationship is explored further in Section 3.2 and 3.3. Fig 2. indicates that the light absorbed by methanol and acetone extracts were almost identical and would imply that the amount and type of OC extracted by the two solvents were similar, as seen in other studies as well (Chen and Bond, 2010; Wang et al., 2014). For some dung samples, the bias for methanol and acetone extracts was close to 0.6 at SSA values of 0.95. These bias values were near to the theoretical prediction of 0.69 – 0.75 by Sun et al. (2007) for particle sizes much smaller than the wavelength of light, even though our size distributions were not significantly smaller than the wavelength of 405 nm. This could indicate that predictions by Sun et al. (2007) are valid for sizes comparable to the wavelength of light as well, but more such observations are necessary to obtain conclusive results. The reason for observed differences in the bias between water and methanol extracts are discussed further in Section 3.3. The differences between the mean values of $b_{abs,OA}/b_{abs,sol}$ ~~$b_{abs,OA}(\lambda)/b_{abs,sol}(\lambda)$~~ at 375 and 405 nm were less than or close to the errors associated with them, hence any trends with wavelength were not explored. In addition to this,

there were no obvious trends that could be explained using fuel type, leading us to not explore trends with fuel type either.

The value of $b_{abs,OA}/b_{abs,sol}$ ~~$b_{abs,OA}(\lambda)/b_{abs,sol}(\lambda)$~~ approached a constant in the measured range of data. A power law ($y = k_0 + k_1 x^{k_2}$) was used to fit the points in Fig. 2, and the corresponding fit parameters, along with root mean square error (RMSE) values, are listed in Table 1. The fit was performed using the curve fitting tool in MATLAB and the RMSE values were calculated in Microsoft Excel. The power law fits were deficient in capturing the true behavior of the bias with SSA but performed better than corresponding mean values and step function curves. The parametrizations presented in this section are representative of laboratory-based biomass burning (BB) aerosol emissions in this study and are provided to mathematically visualize trends in the data. These parametrizations might not be extensible to other emissions and should not be used for determining OA absorption bias in other systems. The contribution of ~~There were large errors associated with the bias for SSA values smaller than 0.7 at 375 nm and smaller than 0.8325 at 405 nm. These large uncertainties at lower SSA are a result of increasing BC mass fractions at these SSA values.~~ BC absorption coefficient~~s~~ to total absorption increase~~s~~ with larger EC ~~concentrations~~ fraction of the aerosol which result~~s~~ in significant errors while extrapolating BC absorption from longer wavelengths ~~due to uncertainties is BC $\AA E$~~. Based on other studies, BC $\AA E$ values range from 0.85 to 1.1 (Lack et al., 2008; Bergstrom et al., 2007; Lan et al., 2013). In Fig. 2, for data points below the perforated lines at SSA values smaller than 0.7 at 375 nm and smaller than 0.825 at 405 nm, the errors due to uncertainties is BC $\AA E$ were greater than 30% and are a result of increasing BC mass fractions at these SSA values. The large uncertainties at lower SSA values indicate that the method described here is best suited to determine $b_{abs,OA}/b_{abs,sol}$ ~~$b_{abs,OA}(\lambda)/b_{abs,sol}(\lambda)$~~ for particles with relatively higher SSA values.

3.2 SSA parametrized with OC/TC

A linear relationship between the SSA and the EC/TC ratio was observed by Pokhrel et al. (2016). To replicate the linear trends observed by Pokhrel et al., we studied the correlation between SSA and OC/TC ratio (which is simply the EC/TC ratio subtracted from 1). Fig. 3 shows the variation in SSA with change in the OC/TC ratio of the aerosol. The OC/TC ratio was determined using the IMPROVE-A TOR protocol with a thermal optical EC/OC analyzer at Sunset laboratories. The data was parametrized using an orthogonal distance regression (ODR) to account for errors in the OC/TC ratio and resulting fits along with data points are plotted in Fig. 3. ODR is different from a standard linear regression as it accounts for errors in both the independent and dependent variables by minimizing least square errors perpendicular to the regression lines rather than vertical errors as in standard linear regression. The ODR fits are linear with RMSE values of 0.04 and 0.02 for wavelengths 375 nm and 405 nm respectively. In Fig. 3, the points corresponding to high OC/TC ratios are associated with SSA values that are close to 1, because pure OC aerosols are predominantly light scattering. The fit yielded SSA values of 0.89 and 0.96 at 375 and 405 nm respectively for pure OA indicating that the fits represent a spectral dependence of absorption which is characteristic of brown carbon optical properties because the SSA values for pure OC are below 1 at both wavelengths and SSA at 375 nm is lower than that at 405 nm. (Chakrabarty et al. 2010).

A linear relation between the SSA and the EC/TC ratio (which is simply the OC/TC ratio subtracted from 1) was also observed by Pokhrel et al. (2016). However, when the data from that study were converted to OC/TC values for comparison, it was noted that the slopes and intercepts of the resulting fits were different from those observed in this study. Table 2 has a list of the slope and intercept of fits for comparable wavelengths in both studies, along with the RMSE for our fit.

A likely reason for dissimilar slopes and intercepts between the two studies could be due to discrepancies in EC/OC ratios obtained using the same temperature protocol. Inter-comparison studies have shown that different labs using the same sample with identical thermal protocols may produce different results (Panteliadis et al., 2015). The instrument bias could be such that obtained OC/TC ratios would have a proportional offset between different instruments leading to similar linear trends but with different slopes which might be the case here. Another plausible reason for the discrepancy could be positive artifacts in EC/OC analysis due to gas phase SVOCs being adsorbed on the quartz surface because of phase ~~portioning~~ partitioning of these compounds in the holding tank. This reason seems less likely due relatively small sampling times for the aerosols. To assess the performance of our parametrizations, we compared our fit to data obtained by Liu et al. (2014) at 405 nm for BB aerosol. Data from the plots w~~as~~ere extracted using Web Plot Digitizer (Rohatgi 2010) and wa~~i~~s plotted with our fit in Fig. 4. We observed that our fits predicted SSA well at OC/TC ratios > 0.7 with a RMSE value of 0.06 compared to 0.08 by Pokhrel et al. (2016) but predictions were worse for 405 nm at lower OC/TC ratios as is also evident from the relatively high SSA value of 0.39 for pure ~~B~~EC obtained using our parametrization ~~at OC/TC ratio of 0~~. Most observations for soot SSA are lower than those predicted by our 405 nm parametrizations (Bond et al., 2013, Schnaiter at al., 2003) with our projections being closer to SSA observed by Radney et al. (2014). Generally, OC/TC ratios are greater than 0.7 for laboratory and field BB (Xie et al., 2019; Akagi et al., 2011; Zhou et al., 2017; Xie et al., 2017) which reduces concerns about underperformance of our fits for 405 nm at low OC/TC ratios. It would be appropriate to use these parametrizations to determine a reasonable range for SSA values rather than use them as a surrogate to determine actual SSA for a given BB aerosol plume. A modification of Fig. 4 which

compares the linear fits by Liu et al. (2014) and Pokhrel et al. (2016) with our parametrizations is provided in the Supplementary Information.

Despite the difference between our fits and those by Pokhrel et al. (2016), a useful conclusion from Fig. 3 is that the OC/TC ratio determined using the IMPROVE-A protocol and SSA of BB aerosol have a linear dependence. This dependence, however, has high variations at OC/TC ratios very close to 1, where fuel type and burn conditions dictate the composition and absorption properties (Chen and Bond, 2010; Budisulistiorini et al., 2017) of organics released and hence a larger range of SSA values exist at those OC/TC ratios. Further studies need to be conducted using more fuels with a variety of distinct size distributions and burn conditions to determine the validity and exact parameters for the fit.

3.3 Absorption bias correlated with OC/TC ratio

Fig. 5 depicts the variation in $b_{abs,OA}/b_{abs,sol}$ ~~$b_{abs,OA}(\lambda)/b_{abs,sol}(\lambda)$~~ for primary OA with different OC/TC ratios. Because the OC/TC ratio and the SSA are well correlated, we expect to see a similar trend for Fig. 5 as in Fig. 2. Similar to Fig. 2, the bias in Fig. 5 increases with decreasing OC/TC ratio and approaches a constant for the three solvents. A power law like the one in Fig. 2 was fit to the data in Fig. 5. The fit parameters for the different solvents at the two wavelengths, along with the RMSE value for each fit, are presented in Table 3. We reiterate that the parametrizations for $b_{abs,OA}/b_{abs,sol}$ ~~$b_{abs,OA}(\lambda)/b_{abs,sol}(\lambda)$~~ as a function of OC/TC ratio depicted here are~~is~~ applicable to our system and should not be used to calculate the bias in other systems. The exclusivity of depicted fit parameters to our system excuses their relatively poor RMSE while representing the bias with OC/TC ratio. The parametrizations are provided to represent some quantitative measure to the data rather than just analyze the trends qualitatively. The large error bars from the Monte Carlo simulations at high EC fractions are mainly due to uncertainties

associated with the BC *ÅÅEAÅE*. At lower OC/TC ratios, the contribution of BC absorption to total particle-phase absorption coefficient is more pronounced, leading to high uncertainties while extrapolating the coefficient to shorter wavelengths. It is apparent from Fig. 5 that these errors in the bias are more prominent at OC/TC ratios below 0.75. The burns with relatively high EC fractions are not representative of typical laboratory or field BB. As mentioned earlier, typical laboratory BB have OC/TC ratios > 0.7 (Xie et al., 2017; Akagi et al., 2011; Pokhrel et al., 2016; Xie et al., 2019) and > 0.9 for field BB (Aurell et al., 2015; Zhou et al., 2017; Xie et al., 2017). Thus, data presented in Fig. 5 with relatively large errors and EC/TC ratios > 0.25 are not representative of typical BB in either laboratory or field settings which may warrant their exclusion from most analysis. We have still included these data points in our plots and Tables but have excluded their use in data analysis due to the high errors associated with them.

In Fig. 5, the difference in magnitude of the bias between methanol/acetone extracts and water extracts increase as EC fraction of the aerosol increases. An increase in the emissions of ELVOCs with increasing EC/OC ratios was observed by Saleh et al. (2014) and we hypothesize that these ELVOCs which have high mass absorption efficiencies (Saleh et al., 2014; Di Lorenzo and Young 2016) could have a lower solubility in water than methanol or acetone which would explain the increasing difference in $b_{abs,OA}/b_{abs,sol}$ values between water and methanol/acetone extracts. Some of the generated ELVOCs might be insoluble in methanol and acetone as well which would lead to the observed increase in the OA absorption bias with decreasing OC fraction of the aerosol. Based on the observed trends, these ELOCs would not be released indefinitely but tend towards a constant above a given EC/OC fraction, mimicking an exponential behavior comparable to observed trends in wavelength dependence for biomass burning OA with EC/OC ratios (Saleh et al., 2014). This would lead to the bias approaching a

constant value (due only to particle size effects) with decreasing OC/TC ratios and in turn the aerosol SSA. Future studies can look at the type and amount of ELVOCs released as a function of the EC/OC ratio of the aerosol and ascertain if their solubility in these solvents is a function of their EC content.

3.4 Variations in ÅAE with solvents and OC/TC ratios

The $AÅE$ ~~AÅE~~ values, for organics extracted in different solvents and those obtained from $b_{abs,OA}$ ~~$b_{abs,OA}$~~ are compared in Table 4. The $AÅE$ ~~$AÅE$~~ values along with the errors for OA measurements were calculated between λ = 375 and 405 nm using the Monte Carlo simulation. The $AÅE$ ~~$AÅE$~~ for O~~A~~C extracts were calculated using Eq. 3 based on $b_{abs,sol}$ ~~$b_{abs,sol}$~~ and corresponding errors were propagated based on uncertainties in ~~the~~ UV-Vis measurements. Consistent with previous studies (Chen and Bond, 2010; Zhang et al., 2013; Liu et al., 2013), the $AÅE$ ~~$AÅE$~~ values of water extracts were larger than the $AÅE$ ~~$AÅE$~~ of acetone and methanol extracts. Experiments by Zhang et al., (2013) observed that polycyclic aromatic hydrocarbons (PAHs) absorbed light at longer wavelengths close to the visible region. Organic ~~compound~~solvents such as methanol have a higher extraction efficiency for these compounds than water leading to higher absorption by methanol extracts at longer wavelengths which results in lower $AÅE$ ~~$AÅE$~~ (Zhang et al., 2013).

The $AÅE$ ~~$AÅE$~~ calculated for OA ranged from 6.9~~87~~ ± 1.7~~3~~ to 15.6~~57~~ ± 0.6~~57~~ (excluding data with OC/TC > 0.75) which are slightly larger than $AÅE$ ~~$AÅE$~~ values reported by most studies (Pokhrel et al., 2016; ~~;~~ Lewis et al., 2008). However, these studies report $AÅE$ ~~AÅE~~ values in the visible range, which might be lower than aerosol $AÅE$ ~~$AÅE$~~ values in the UV range as observed by Chen and Bond (2010) for OA extracts. The range of $AÅE$ ~~$AÅE$~~ observed for water, acetone and methanol

extracts were similar to those observed by Chen and Bond (2010). A t-test for data presented in Table 4 shows that *AÅE* ~~*AÅE*~~ values for OA were greater than their solution phase counterparts for both methanol (N = 17, $p = 0.0007$) and acetone (N = 17, $p = 0.0002$). The difference in *AÅE* ~~*AÅE*~~ of OA and water extracts were statistically insignificant (N = 17, $p = 0.25$), but these differences were statistically significant at OC/TC ratios ≥ 0.9 (N = 12, $p < 0.05$) where uncertainties due to BC absorption are lower. The reason for these differences could be a combination of artifacts due to inefficient extraction of organics absorbing light at lower wavelengths and the absence of size dependent absorption in the solvent phase which might not capture effects of enhanced particle phase absorption at lower wavelengths. These bulk solvent measurements of *AÅE* ~~*AÅE*~~ suggest that they might not be representative of spectral dependence of OC in the particle phase, and future studies and models should be cautious while using *AÅE* ~~*AÅE*~~ data from solvent-phase measurements to be representative of the particle phase.

3.54 Scaling factors based on Mie ~~C~~calculations

To check the reproducibility of the conventionally used correction factor of 2, ~~T~~the absorption coefficient determined from the bulk solvent absorbance using Eq. (1) was compared to absorption coefficients calculated using Mie theory for three samples of smoldering sage. The EC/OC analysis (IMPROVE-A protocol) determined that these samples consisted purely of OC, and because the SMPS measurements and TOC analysis were only performed on the first set of samples, the three samples of sage were considered optimum for ~~the~~ Mie calculations.

The Mie based scaling factors for converting solution phase absorption coefficients to particulate absorption for the three samples are presented in Table 5. TOC and EC/OC analysis indicated that a similar fraction of organics at 61 ± 2% were extracted from all three samples. The Mie calculated

scaling factors at 375 nm and 405 nm are close to 2 as observed in previous studies (Liu et al., 2013; Washenfelder et al., 2015) indicating that the conventional technique provides reproducible results. The values for these scaling factor vary from ~~1.99~~2 to 2.1~~05~~ at 375 nm and 2.2~~15~~ to 2.3~~29~~ at 405 nm. However, it is important to note that these scaling factors ~~are~~ were not representative of actual biases for determining OA absorption from solution phase as observed in Table 5. Thus, while a Mie based correction factor of 2 can be duplicated, it ~~cannot be used for all conditions~~is not representative of actual biases~~,~~ as also corroborated by observations from Fig. 2 and Fig. 5. We ~~advise~~ recommend future studies~~researchers~~ to use caution and judgement when using *a priori* scaling factors ~~avoid using such scaling factors~~ for determining OA absorption ~~without exact knowledge of OC extraction efficiencies and particle size distributions.~~using solvent extraction techniques.

4 Conclusions

Under controlled laboratory conditions, we determined artifacts associated with optical properties of the solvent phase as compared to particle phase counterparts for ~~primary~~ fresh OA emissions from biomass combustion. We combusted a range of different wildland fuels under different combustion conditions, generating a span of different SSA and OC/TC values. The SSA values ranged from 0.55 to 0.87 at 375 nm, and from 0.69 to 0.95 at 405 nm, the OC/TC values ranged from 0.55 to 1. We observed an increasing difference in $b_{abs,OA}/b_{abs,sol}$ ~~$b_{abs,OA}/b_{abs,sol}$~~ for water and methanol extracts with increasing EC fraction of the aerosol. The decrease in ~~water extracted~~ absorption by water extracts with decreasing OC/TC ratios was hypothesized to occur due to a decrease in extraction of ELVOC or similar compounds with high mass absorption efficiencies by water. We also demonstrated that the SSA and OC/TC ratios can be well parametrized with a linear fit that captures the effects of brown carbon aerosol. We also determined that bulk solvent

measurements of $\AA E$ are not representative of spectral dependence of OC in the particle phase. Finally, ~~W~~we analyzed the validity and reproducibility of the conventionally used scaling factor of 2 for determining OA absorption coefficients from water extracts of organics and noted that, while the factor is reproducible, its use can misrepresent OA absorption coefficients. We recommend that future studies use caution while applying ~~not use such~~ a priori scaling factors to their systems as these factors might not be ~~without knowledge of the OC extraction efficiency and particle size distributions as these scaling factors might not be~~ extensible to ~~organic aerosol~~OA emissions from all combustion processes. A comprehensive technique which improves extraction efficiency with accurate knowledge of particle size distributions is necessary to determine correct scaling relations.

For future experiments, a better technique to quantify BC absorption at lower wavelengths, such as a thermodenuder to strip off all OC, or a single particle soot photometer along with core-shell Mie calculations can be used to determine BC absorption ~~to~~and decrease uncertainties ~~for~~ related to BC absorption observed during experiments using this technique. Zhang et al. (2013) observed lower $\AA E$ ~~$A\AA E$~~ for WSOC from a particle into liquid sampler (PILS) than for methanol extracts. The hypothesis was that the highly dilute environment in PILS increased dissolution of organics in water. This suggests that extraction of organics can be increased by heavily diluting the samples. This can be combined with highly accurate spectrometers similar to the technique used by Hecobian et al. (2010) to reduce some of the biases due to incomplete OA extraction.

Author Contributions

RKC conceived of this study and designed the experiments. SB and WMH collected the fuels for the experiments and performed EC/OC analysis on the sampled filters. NJS and AP carried out the

experiments ~~and analysed the data~~. NJS analysed the data and prepared the manuscript with input from all co-authors.

Acknowledgements

This work was partially supported by the National Science Foundation under Grant No. AGS1455215, NASA ROSES under Grant No. NNX15AI66G.

References

Akagi, S., Yokelson, R. J., Wiedinmyer, C., Alvarado, M., Reid, J., Karl, T., Crounse, J., and Wennberg, P.: Emission factors for open and domestic biomass burning for use in atmospheric models, Atmos. Chem. Phys., 11, 4039-4072, https://doi.org/10.5194/acp-11-4039-2011, 2011.

Alexander, D. T., Crozier, P. A., and Anderson, J. R.: Brown carbon spheres in East Asian outflow and their optical properties, Science, 321, 833-836, https://doi.org/10.1126/science.1155296, 2008.

Andreae, M., and Gelencsér, A.: Black carbon or brown carbon? The nature of light-absorbing carbonaceous aerosols, Atmos. Chem. Phys., 6, 3131-3148, https://doi.org/10.5194/acp-6-3131-2006, 2006.

Arnott, W., Moosmüller, H., Sheridan, P., Ogren, J., Raspet, R., Slaton, W., Hand, J., Kreidenweis, S., and Collett Jr, J.: Photoacoustic and filter-based ambient aerosol light absorption measurements: Instrument comparisons and the role of relative humidity, J. Geophys. Res-Atmos., 108, AAC 15-1-AAC 15-11, https://doi.org/10.1029/2002JD002165, 2003.

Arnott, W. P., Hamasha, K., Moosmüller, H., Sheridan, P. J., and Ogren, J. A.: Towards aerosol light-absorption measurements with a 7-wavelength aethalometer: Evaluation with a photoacoustic instrument and 3-wavelength nephelometer, Aerosol Sci. Tech., 39, 17-29, https://doi.org/10.1080/027868290901972, 2005.

Arola, A., Schuster, G., Myhre, G., Kazadzis, S., Dey, S., and Tripathi, S.: Inferring absorbing organic carbon content from AERONET data, Atmos. Chem. Phys., 11, 215-225, https://doi.org/10.5194/acp-11-215-2011, 2011.

Aurell, J., Gullett, B. K., and Tabor, D.: Emissions from southeastern US Grasslands and pine savannas: Comparison of aerial and ground field measurements with laboratory burns, Atmos. Environ., 111, 170-178, https://doi.org/10.1016/j.atmosenv.2015.03.001, 2015.

Bahadur, R., Praveen, P. S., Xu, Y., and Ramanathan, V.: Solar absorption by elemental and brown carbon determined from spectral observations, P. Nat. Acad. Sci., 109 (43), 17366-17371, https://doi.org/10.1073/pnas.1205910109, 2012.

Bergstrom, R. W., Pilewskie, P., Russell, P. B., Redemann, J., Bond, T. C., Quinn, P. K., and Sierau, B.: Spectral absorption properties of atmospheric aerosols, Atmos. Chem. Phys., 7, 5937-5943, https://doi.org/10.5194/acp-7-5937-2007, 2007.

Bond, T. C., Doherty, S. J., Fahey, D., Forster, P., Berntsen, T., DeAngelo, B., Flanner, M., Ghan, S., Kärcher, B., and Koch, D.: Bounding the role of black carbon in the climate system: A scientific assessment, J. Geophys. Res-Atmos., 118, 5380-5552 , https://doi:10.1002/jgrd.50171, 2013.

Bosch, C., Andersson, A., Kirillova, E. N., Budhavant, K., Tiwari, S., Praveen, P., Russell, L. M., Beres, N. D., Ramanathan, V., and Gustafsson, Ö.: Source-diagnostic dual-isotope composition and optical properties of water-soluble organic carbon and elemental carbon in the South Asian outflow intercepted over the Indian Ocean, J. Geophys. Res-Atmos., 119, 11,743-711,759, https://doi:10.1002/2014JD022127, 2014.

Budisulistiorini, S. H., Riva, M., Williams, M., Chen, J., Itoh, M., Surratt, J. D., and Kuwata, M.: Light-absorbing brown carbon aerosol constituents from combustion of Indonesian peat and biomass, Environ. Sci. & Technol., 51, 4415-4423, https://doi.org/10.1021/acs.est.7b00397, 2017.

Chakrabarty, R., Moosmüller, H., Chen, L.-W., Lewis, K., Arnott, W., Mazzoleni, C., Dubey, M., Wold, C., Hao, W., and Kreidenweis, S.: Brown carbon in tar balls from smoldering biomass combustion, Atmos. Chem. Phys., 10, 6363-6370, https://doi.org/10.5194/acp-10-6363-2010, 2010.

Chen, Y., and Bond, T.: Light absorption by organic carbon from wood combustion, Atmos. Chem. Phys., 10, 1773-1787, https://doi.org/10.5194/acp-10-1773-2010, 2010.

Cheng, Y., He, K.-b., Du, Z.-y., Engling, G., Liu, J.-m., Ma, Y.-l., Zheng, M., and Weber, R. J.: The characteristics of brown carbon aerosol during winter in Beijing, Atmos. Environ., 127, 355-364, https://doi.org/10.1016/j.atmosenv.2015.12.035, 2016.

Chow, J. C., Watson, J. G., Chen, L.-W. A., Chang, M. O., Robinson, N. F., Trimble, D., and Kohl, S.: The IMPROVE_A temperature protocol for thermal/optical carbon analysis: maintaining consistency with a long-term database, J. Air Waste Manage., 57, 1014-1023, https://doi.org/10.3155/1047-3289.57.9.1014, 2007a.

Chow, J. C., Yu, J. Z., Watson, J. G., Hang Ho, S. S., Bohannan, T. L., Hays, M. D., and Fung, K. K.: The application of thermal methods for determining chemical composition of carbonaceous aerosols: A review, J. Environ. Sci. Heal. A, 42, 1521-1541, https://doi.org/10.1080/10934520701513365, 2007b.

Di Lorenzo, R. A., and Young, C. J.: Size separation method for absorption characterization in brown carbon: Application to an aged biomass burning sample, Geophys. Res. Lett., 43, 458-465, https://doi.org/10.1002/2015GL066954. 2016.

Feng, Y., Ramanathan, V., and Kotamarthi, V.: Brown carbon: a significant atmospheric absorber of solar radiation?, Atmos. Chem. Phys., 13, 8607-8621, https://doi.org/10.5194/acp-13-8607-2013, 2013.

Hecobian, A., Zhang, X., Zheng, M., Frank, N., Edgerton, E. S., and Weber, R. J.: Water-Soluble Organic Aerosol material and the light-absorption characteristics of aqueous extracts measured

over the Southeastern United States, Atmos. Chem. Phys., 10, 5965-5977, https://doi.org/10.5194/acp-10-5965-2010, 2010.

Husain, L., Dutkiewicz, V. A., Khan, A., and Ghauri, B. M.: Characterization of carbonaceous aerosols in urban air, Atmos. Environ., 41, 6872-6883, https://doi.org/10.1016/j.atmosenv.2007.04.037, 2007. Akagi, S., Yokelson, R. J., Wiedinmyer, C., Alvarado, M., Reid, J., Karl, T., . . . Wennberg, P. (2011). Emission factors for open and domestic biomass burning for use in atmospheric models. Atmospheric Chemistry and Physics, 11(9), 4039-4072.

Alexander, D. T., Crozier, P. A., & Anderson, J. R. (2008). Brown carbon spheres in East Asian outflow and their optical properties. Science, 321(5890), 833-836.

Andreae, M., & Gelencsér, A. (2006). Black carbon or brown carbon? The nature of light-absorbing carbonaceous aerosols. Atmospheric Chemistry and Physics, 6(10), 3131-3148.

Arnott, W., Moosmüller, H., Sheridan, P., Ogren, J., Raspet, R., Slaton, W., . . . Collett Jr, J. (2003). Photoacoustic and filter-based ambient aerosol light absorption measurements: Instrument comparisons and the role of relative humidity. Journal of Geophysical Research: Atmospheres, 108(D1), AAC 15-11-AAC 15-11.

Arnott, W. P., Hamasha, K., Moosmüller, H., Sheridan, P. J., & Ogren, J. A. (2005). Towards aerosol light-absorption measurements with a 7-wavelength aethalometer: Evaluation with a photoacoustic instrument and 3-wavelength nephelometer. Aerosol Science and Technology, 39(1), 17-29.

Arola, A., Schuster, G., Myhre, G., Kazadzis, S., Dey, S., & Tripathi, S. (2011). Inferring absorbing organic carbon content from AERONET data. Atmospheric Chemistry and Physics, 11(1), 215-225.

Aurell, J., Gullett, B. K., & Tabor, D. (2015). Emissions from southeastern US Grasslands and pine savannas: Comparison of aerial and ground field measurements with laboratory burns. Atmospheric environment, 111, 170-178.

Bahadur, R., Praveen, P. S., Xu, Y., & Ramanathan, V. (2012). Solar absorption by elemental and brown carbon determined from spectral observations. Proceedings of the National Academy of Sciences, 201205910.

Bergstrom, R. W., Pilewskie, P., Russell, P. B., Redemann, J., Bond, T. C., Quinn, P. K., & Sierau, B. (2007). Spectral absorption properties of atmospheric aerosols. Atmospheric Chemistry and Physics, 7(23), 5937-5943.

Bond, T. C., Doherty, S. J., Fahey, D., Forster, P., Berntsen, T., DeAngelo, B., . . . Koch, D. (2013). Bounding the role of black carbon in the climate system: A scientific assessment. Journal of Geophysical Research: Atmospheres, 118(11), 5380-5552.

595 Bosch, C., Andersson, A., Kirillova, E. N., Budhavant, K., Tiwari, S., Praveen, P., . . . Gustafsson,
596 Ö. (2014). Source-diagnostic dual-isotope composition and optical properties of water-soluble
597 organic carbon and elemental carbon in the South Asian outflow intercepted over the Indian Ocean.
598 Journal of Geophysical Research: Atmospheres, 119(20), 11,743-711,759.

599 Budisulistiorini, S. H., Riva, M., Williams, M., Chen, J., Itoh, M., Surratt, J. D., & Kuwata, M.
600 (2017). Light-absorbing brown carbon aerosol constituents from combustion of Indonesian peat
601 and biomass. Environmental science & technology, 51(8), 4415-4423.

602 Chakrabarty, R., Moosmüller, H., Chen, L.-W., Lewis, K., Arnott, W., Mazzoleni, C., . . .
603 Kreidenweis, S. (2010). Brown carbon in tar balls from smoldering biomass combustion.
604 Atmospheric Chemistry and Physics, 10(13), 6363-6370.

605 Chen, Y., & Bond, T. (2010). Light absorption by organic carbon from wood combustion.
606 Atmospheric Chemistry and Physics, 10(4), 1773-1787.

607 Cheng, Y., He, K. b., Du, Z. y., Engling, G., Liu, J. m., Ma, Y. l., . . . Weber, R. J. (2016). The
608 characteristics of brown carbon aerosol during winter in Beijing. Atmospheric environment, 127,
609 355-364.

610 Chow, J. C., Watson, J. G., Chen, L.-W. A., Chang, M. O., Robinson, N. F., Trimble, D., & Kohl,
611 S. (2007). The IMPROVE_A temperature protocol for thermal/optical carbon analysis:
612 maintaining consistency with a long-term database. Journal of the Air & Waste Management
613 Association, 57(9), 1014-1023.

614 Chow, J. C., Yu, J. Z., Watson, J. G., Hang Ho, S. S., Bohannan, T. L., Hays, M. D., & Fung, K.
615 K. (2007). The application of thermal methods for determining chemical composition of
616 carbonaceous aerosols: A review. Journal of Environmental Science and Health Part A, 42(11),
617 1521-1541.

618 Di Lorenzo, R. A., & Young, C. J. (2016). Size separation method for absorption characterization
619 in brown carbon: Application to an aged biomass burning sample. Geophysical Research Letters,
620 43(1), 458-465.

621 Feng, Y., Ramanathan, V., & Kotamarthi, V. (2013). Brown carbon: a significant atmospheric
622 absorber of solar radiation? Atmospheric Chemistry and Physics, 13(17), 8607-8621.

623 Hecobian, A., Zhang, X., Zheng, M., Frank, N., Edgerton, E. S., & Weber, R. J. (2010). Water-
624 Soluble Organic Aerosol material and the light-absorption characteristics of aqueous extracts
625 measured over the Southeastern United States. Atmospheric Chemistry and Physics, 10(13), 5965-
626 5977.

627 Husain, L., Dutkiewicz, V. A., Khan, A., & Ghauri, B. M. (2007). Characterization of
628 carbonaceous aerosols in urban air. Atmospheric environment, 41(32), 6872-6883.

IPCC: Climate Change: The Physical Science Basis, Contribution of Working Group I to the UN IPCC's 5th Assessment Report, Cambridge University Press, New York, USA, 2013.

Kim, H., Kim, J. Y., Jin, H. C., Lee, J. Y., and Lee, S. P.: Seasonal variations in the light-absorbing properties of water-soluble and insoluble organic aerosols in Seoul, Korea, Atmos. Environ., 129, 234-242, https://doi.org/10.1016/j.atmosenv.2016.01.042, 2016.

Kirchstetter, T. W., Novakov, T., and Hobbs, P. V.: Evidence that the spectral dependence of light absorption by aerosols is affected by organic carbon, J. Geophys. Res-Atmos., 109, D21208 https://doi.org/10.1029/2004JD004999, 2004.

Kirchstetter, T., and Thatcher, T.: Contribution of organic carbon to wood smoke particulate matter absorption of solar radiation, Atmos. Chem. Phys., 12, 6067-6072, https://doi.org/10.5194/acp-12-6067-2012, 2012.

Kirillova, E. N., Andersson, A., Han, J., Lee, M., and Gustafsson, Ö.: Sources and light absorption of water-soluble organic carbon aerosols in the outflow from northern China, Atmos. Chem. Phys., 14, 1413-1422, https://doi.org/10.5194/acp-14-1413-2014, 2014a.

Kirillova, E. N., Andersson, A., Tiwari, S., Srivastava, A. K., Bisht, D. S., and Gustafsson, Ö.: Water-soluble organic carbon aerosols during a full New Delhi winter: Isotope-based source apportionment and optical properties, J. Geophys. Res-Atmos., 119, 3476-3485, https://doi:10.1002/2013JD020041, 2014b.

Lack, D. A., Lovejoy, E. R., Baynard, T., Pettersson, A., and Ravishankara, A.: Aerosol absorption measurement using photoacoustic spectroscopy: Sensitivity, calibration, and uncertainty developments, Aerosol Sci. Tech., 40, 697-708, https://doi.org/10.1080/02786820600803917, 2006.

Lack, D. A., Cappa, C. D., Covert, D. S., Baynard, T., Massoli, P., Sierau, B., Bates, T. S., Quinn, P. K., Lovejoy, E. R., and Ravishankara, A.: Bias in filter-based aerosol light absorption measurements due to organic aerosol loading: Evidence from ambient measurements, Aerosol Sci. Tech., 42, 1033-1041, https://doi.org/10.1080/02786820802389277, 2008.

Lan, Z.-J., Huang, X.-F., Yu, K.-Y., Sun, T.-L., Zeng, L.-W., and Hu, M.: Light absorption of black carbon aerosol and its enhancement by mixing state in an urban atmosphere in South China, Atmos. Environ., 69, 118-123, https://doi.org/10.1016/j.atmosenv.2012.12.009, 2013.

Lin, G., Penner, J. E., Flanner, M. G., Sillman, S., Xu, L., and Zhou, C.: Radiative forcing of organic aerosol in the atmosphere and on snow: Effects of SOA and brown carbon, J. Geophys. Res-Atmos., 119, 7453-7476, https://doi.org/10.1002/2013JD021186, 2014.

Liu, J., Bergin, M., Guo, H., King, L., Kotra, N., Edgerton, E., and Weber, R.: Size-resolved measurements of brown carbon in water and methanol extracts and estimates of their contribution

to ambient fine-particle light absorption, Atmos. Chem. Phys., 13, 12389-12404, https://doi.org/10.5194/acp-13-12389-2013, 2013.

Liu, S., Aiken, A. C., Arata, C., Dubey, M. K., Stockwell, C. E., Yokelson, R. J., Stone, E. A., Jayarathne, T., Robinson, A. L., and DeMott, P. J.: Aerosol single scattering albedo dependence on biomass combustion efficiency: Laboratory and field studies, Geophys. Res. Lett., 41, 742-748, https://doi.org/10.1002/2013GL058392, 2014.

Liu, J., Lin, P., Laskin, A., Laskin, J., Kathmann, S. M., Wise, M., Caylor, R., Imholt, F., Selimovic, V., and Shilling, J. E.: Optical properties and aging of light-absorbing secondary organic aerosol, Atmos. Chem. Phys., 16, 12815-12827, https://doi.org/10.5194/acp-16-12815-2016, 2016.

Mo, Y., Li, J., Liu, J., Zhong, G., Cheng, Z., Tian, C., Chen, Y., and Zhang, G.: The influence of solvent and pH on determination of the light absorption properties of water-soluble brown carbon, Atmos. Environ., 161, 90-98, https://doi.org/10.1016/j.atmosenv.2017.04.037, 2017.

Moosmüller, H., Chakrabarty, R., and Arnott, W.: Aerosol light absorption and its measurement: A review, J. Quant. Spectrosc. Ra., 110, 844-878, https://doi.org/10.1016/j.jqsrt.2009.02.035, 2009.

Moosmüller, H., Chakrabarty, R., Ehlers, K., and Arnott, W.: Absorption Ångström coefficient, brown carbon, and aerosols: basic concepts, bulk matter, and spherical particles, Atmos. Chem. Phys., 11, 1217-1225, https://doi.org/10.5194/acp-11-1217-2011, 2011.

Mutzel, A., Rodigast, M., Iinuma, Y., Böge, O., and Herrmann, H.: An improved method for the quantification of SOA bound peroxides, Atmos. Environ., 67, 365-369, https://doi.org/10.1016/j.atmosenv.2012.11.012, 2013.

Panteliadis, P., Hafkenscheid, T., Cary, B., Diapouli, E., Fischer, A., Favez, O., Quincey, P., Viana, M., Hitzenberger, R., Vecchi, R., Saraga, D., Sciare, J., Jaffrezo, J. L., John, A., Schwarz, J., Giannoni, M., Novak, J., Karanasiou, A., Fermo, P., and Maenhaut, W.: ECOC comparison exercise with identical thermal protocols after temperature offset correction - instrument diagnostics by in-depth evaluation of operational parameters, Atmos. Meas. Tech., 8, 779-792, https://doi.org/10.5194/amt-8-779-2015, 2015.

Phillips, S. M., and Smith, G. D.: Spectroscopic comparison of water-and methanol-soluble brown carbon particulate matter, Aerosol Sci. Tech., 51, 1113-1121, https://doi.org/10.1080/02786826.2017.1334109, 2017.

Pokhrel, R. P., Wagner, N. L., Langridge, J. M., Lack, D. A., Jayarathne, T., Stone, E. A., Stockwell, C. E., Yokelson, R. J., and Murphy, S. M.: Parameterization of single-scattering albedo (SSA) and absorption Ångström exponent (AAE) with EC/OC for aerosol emissions from biomass burning, Atmos. Chem. Phys., 16, 9549-9561, https://doi.org/10.5194/acp-16-9549-2016, 2016.

Radney, J. G., You, R., Ma, X., Conny, J. M., Zachariah, M. R., Hodges, J. T., and Zangmeister, C. D.: Dependence of soot optical properties on particle morphology: measurements and model comparisons, Environ. Sci. Technol., 48, 3169-3176, https://doi.org/10.1021/es4041804, 2014.

Ramanathan, V., and Carmichael, G.: Global and regional climate changes due to black carbon, Nat. Geosci., 1, 221–227, https://doi.org/10.1038/ngeo156, 2008.

Kim, H., Kim, J. Y., Jin, H. C., Lee, J. Y., & Lee, S. P. (2016). Seasonal variations in the light-absorbing properties of water-soluble and insoluble organic aerosols in Seoul, Korea. Atmospheric environment, 129, 234-242.

Kirchstetter, T. W., Novakov, T., & Hobbs, P. V. (2004). Evidence that the spectral dependence of light absorption by aerosols is affected by organic carbon. Journal of Geophysical Research: Atmospheres, 109(D21).

Kirchstetter, T., & Thatcher, T. (2012). Contribution of organic carbon to wood smoke particulate matter absorption of solar radiation. Atmospheric Chemistry and Physics, 12(14), 6067-6072.

Kirillova, E. N., Andersson, A., Han, J., Lee, M., & Gustafsson, Ö. (2014a). Sources and light absorption of water-soluble organic carbon aerosols in the outflow from northern China. Atmospheric Chemistry and Physics, 14(3), 1413-1422.

Kirillova, E. N., Andersson, A., Tiwari, S., Srivastava, A. K., Bisht, D. S., & Gustafsson, Ö. (2014b). Water-soluble organic carbon aerosols during a full New Delhi winter: Isotope-based source apportionment and optical properties. Journal of Geophysical Research: Atmospheres, 119(6), 3476-3485.

Lack, D. A., Lovejoy, E. R., Baynard, T., Pettersson, A., & Ravishankara, A. (2006). Aerosol absorption measurement using photoacoustic spectroscopy: Sensitivity, calibration, and uncertainty developments. Aerosol Science and Technology, 40(9), 697-708.

Lin, G., Penner, J. E., Flanner, M. G., Sillman, S., Xu, L., & Zhou, C. (2014). Radiative forcing of organic aerosol in the atmosphere and on snow: Effects of SOA and brown carbon. Journal of Geophysical Research: Atmospheres, 119(12), 7453-7476.

Liu, J., Bergin, M., Guo, H., King, L., Kotra, N., Edgerton, E., & Weber, R. (2013). Size-resolved measurements of brown carbon in water and methanol extracts and estimates of their contribution to ambient fine-particle light absorption. Atmospheric Chemistry and Physics, 13(24), 12389-12404.

Liu, J., Lin, P., Laskin, A., Laskin, J., Kathmann, S. M., Wise, M., . . . Shilling, J. E. (2016). Optical properties and aging of light-absorbing secondary organic aerosol. Atmospheric Chemistry and Physics, 16(19), 12815-12827.

Liu, S., Aiken, A. C., Arata, C., Dubey, M. K., Stockwell, C. E., Yokelson, R. J., . . . DeMott, P. J. (2014). Aerosol single scattering albedo dependence on biomass combustion efficiency: Laboratory and field studies. Geophysical Research Letters, 41(2), 742-748.

Mo, Y., Li, J., Liu, J., Zhong, G., Cheng, Z., Tian, C., . . . Zhang, G. (2017). The influence of solvent and pH on determination of the light absorption properties of water-soluble brown carbon. Atmospheric environment, 161, 90-98.

Moosmüller, H., Chakrabarty, R., & Arnott, W. (2009). Aerosol light absorption and its measurement: A review. Journal of Quantitative Spectroscopy and Radiative Transfer, 110(11), 844-878.

Moosmüller, H., Chakrabarty, R., Ehlers, K., & Arnott, W. (2011). Absorption Ångström coefficient, brown carbon, and aerosols: basic concepts, bulk matter, and spherical particles. Atmospheric Chemistry and Physics, 11(3), 1217-1225.

Panteliadis, P., Hafkenscheid, T., Cary, B., Diapouli, E., Fischer, A., Favez, O., . . . Vecchi, R. (2015). ECOC comparison exercise with identical thermal protocols after temperature offset correction: instrument diagnostics by in-depth evaluation of operational parameters.

Phillips, S. M., & Smith, G. D. (2017). Spectroscopic comparison of water-and methanol-soluble brown carbon particulate matter. Aerosol Science and Technology, 51(9), 1113-1121.

Pokhrel, R. P., Wagner, N. L., Langridge, J. M., Lack, D. A., Jayarathne, T., Stone, E. A., . . . Murphy, S. M. (2016). Parameterization of single-scattering albedo (SSA) and absorption Ångström exponent (AAE) with EC/OC for aerosol emissions from biomass burning. Atmospheric Chemistry and Physics, 16(15), 9549-9561.

Ramanathan, V., & Carmichael, G. (2008). Global and regional climate changes due to black carbon. Nature Geoscience, 1(4), 221.

Rohatgi, A. :(2012) WebPlotDigitalizer: HTML5 based online tool to extract numerical data from plot images. URL http://arohatgi.info/WebPlotDigitizer/app, 2012.

Saleh, R., Robinson, E. S., Tkacik, D. S., Ahern, A. T., Liu, S., Aiken, A. C., Sullivan, R. C., Presto, A. A., Dubey, M. K., and Yokelson, R. J.: Brownness of organics in aerosols from biomass burning linked to their black carbon content, Nat. Geosci., 7, 647–650, https://doi.org/10.1038/ngeo2220, 2014.

Saleh, R., Marks, M., Heo, J., Adams, P. J., Donahue, N. M., and Robinson, A. L.: Contribution of brown carbon and lensing to the direct radiative effect of carbonaceous aerosols from biomass and biofuel burning emissions, J. Geophys. Res-Atmos., 120, 10,285–10,296, https://doi:10.1002/2015JD023697., 2015.

764 Schnaiter, M., Horvath, H., Möhler, O., Naumann, K.-H., Saathoff, H., and Schöck, O.: UV-VIS-
765 NIR spectral optical properties of soot and soot-containing aerosols, J. Aerosol Sci., 34, 1421-
766 1444, https://doi.org/10.1016/S0021-8502(03)00361-6, 2003.

767 Shen, Z., Lei, Y., Zhang, L., Zhang, Q., Zeng, Y., Tao, J., Zhu, C., Cao, J., Xu, H., and Liu, S.:
768 Methanol extracted brown carbon in PM 2.5 over Xi'an, China: seasonal variation of optical
769 properties and sources identification, Aerosol Sci. Eng., 1, 57-65, https://doi.org/10.1007/s41810-
770 017-0007-z, 2017.

771 Sorensen, C.: Light scattering by fractal aggregates: a review, Aerosol Sci. Tech., 35, 648-687,
772 https://doi.org/10.1080/02786820117868, 2001.

773 Sumlin, B. J., Heinson, W. R., and Chakrabarty, R. K.: Retrieving the aerosol complex refractive
774 index using PyMieScatt: A Mie computational package with visualization capabilities, J. Quant.
775 Spectrosc. Ra., 205, 127-134, https://doi.org/10.1016/j.jqsrt.2017.10.012, 2018a.

776 Sumlin, B. J., Heinson, Y. W., Shetty, N., Pandey, A., Pattison, R. S., Baker, S., Hao, W. M., and
777 Chakrabarty, R. K.: UV–Vis–IR spectral complex refractive indices and optical properties of
778 brown carbon aerosol from biomass burning, J. Quant. Spectrosc. Ra., 206, 392-398,
779 https://doi.org/10.1016/j.jqsrt.2017.12.009, 2018b.

780 Sun, H., Biedermann, L., and Bond, T. C.: Color of brown carbon: A model for ultraviolet and
781 visible light absorption by organic carbon aerosol, Geophys. Res. Lett., 34, L17813,
782 https://doi.org/10.1029/2007GL029797, 2007.

783 Wang, X., Heald, C., Ridley, D., Schwarz, J., Spackman, J., Perring, A., Coe, H., Liu, D., and
784 Clarke, A.: Exploiting simultaneous observational constraints on mass and absorption to estimate
785 the global direct radiative forcing of black carbon and brown carbon, Atmos. Chem. Phys., 14,
786 10989-11010, https://doi.org/10.5194/acp-14-10989-2014, 2014.

787 Wang, X., Heald, C. L., Liu, J., Weber, R. J., Campuzano-Jost, P., Jimenez, J. L., Schwarz, J. P.,
788 and Perring, A. E.: Exploring the observational constraints on the simulation of brown carbon,
789 Atmos. Chem. Phys., 18, 635-653, 10.5194/acp-18-635-2018, https://doi.org/10.5194/acp-18-635-
790 2018, 2018.

791 Washenfelder, R., Attwood, A., Brock, C., Guo, H., Xu, L., Weber, R., Ng, N., Allen, H., Ayres,
792 B., and Baumann, K.: Biomass burning dominates brown carbon absorption in the rural
793 southeastern United States, Geophys. Res. Lett., 42, 653-664,
794 https://doi.org/10.1002/2014GL062444, 2015.

795 Xie, M., Hays, M. D., and Holder, A. L.: Light-absorbing organic carbon from prescribed and
796 laboratory biomass burning and gasoline vehicle emissions, Sci. Rep., 7, 7318,
797 https://doi.org/10.1038/s41598-017-06981-8, 2017.

Xie, M., Chen, X., Hays, M. D., and Holder, A. L.: Composition and light absorption of N-containing aromatic compounds in organic aerosols from laboratory biomass burning, Atmos. Chem. Phys., 19, 2899-2915, https://doi.org/10.5194/acp-19-2899-2019, 2019.

Yang, M., Howell, S., Zhuang, J., and Huebert, B.: Attribution of aerosol light absorption to black carbon, brown carbon, and dust in China–interpretations of atmospheric measurements during EAST-AIRE, Atmos. Chem. Phys., 9, 2035-2050, https://doi.org/10.5194/acp-9-2035-2009, 2009.

Zhang, X., Wang, Y., Zhang, X., Guo, W., and Gong, S.: Carbonaceous aerosol composition over various regions of China during 2006, J. Geophys. Res-Atmos., 113, D14111, https://doi.org/10.1029/2007JD009525, 2008.

Zhang, X., Lin, Y.-H., Surratt, J. D., and Weber, R. J.: Sources, composition and absorption Ångstrom exponent of light-absorbing organic components in aerosol extracts from the Los Angeles Basin, Environ. Sci. & Technol., 47, 3685-3693, https://doi.org/10.1021/es305047b, 2013.

Zhang, Y., Forrister, H., Liu, J., Dibb, J., Anderson, B., Schwarz, J. P., Perring, A. E., Jimenez, J. L., Campuzano-Jost, P., and Wang, Y.: Top-of-atmosphere radiative forcing affected by brown carbon in the upper troposphere, Nat. Geosci., 10, 486–489, https://doi.org/10.1038/ngeo2960, 2017.

Zhou, Y., Xing, X., Lang, J., Chen, D., Cheng, S., Lin, W., Xiao, W., and Liu, C.: A comprehensive biomass burning emission inventory with high spatial and temporal resolution in China, Atmos. Chem. Phys., 17, 2839-2864, https://doi.org/10.5194/acp-17-2839-2017, 2017. Saleh, R., Marks, M., Heo, J., Adams, P. J., Donahue, N. M., & Robinson, A. L. (2015). Contribution of brown carbon and lensing to the direct radiative effect of carbonaceous aerosols from biomass and biofuel burning emissions. Journal of Geophysical Research: Atmospheres, 120(19).

Saleh, R., Robinson, E. S., Tkacik, D. S., Ahern, A. T., Liu, S., Aiken, A. C., . . . Yokelson, R. J. (2014). Brownness of organics in aerosols from biomass burning linked to their black carbon content. Nature Geoscience, 7(9), 647.

Schnaiter, M., Horvath, H., Möhler, O., Naumann, K.-H., Saathoff, H., & Schöck, O. (2003). UV-VIS-NIR spectral optical properties of soot and soot-containing aerosols. Journal of Aerosol Science, 34(10), 1421-1444.

Shen, Z., Lei, Y., Zhang, L., Zhang, Q., Zeng, Y., Tao, J., . . . Liu, S. (2017). Methanol extracted brown carbon in PM 2.5 over Xi'an, China: seasonal variation of optical properties and sources identification. Aerosol Science and Engineering, 1(2), 57-65.

Sorensen, C. (2001). Light scattering by fractal aggregates: a review. Aerosol Science & Technology, 35(2), 648-687.

Sumlin, B. J., Heinson, W. R., & Chakrabarty, R. K. (2018a). Retrieving the aerosol complex refractive index using PyMieScatt: A Mie computational package with visualization capabilities. Journal of Quantitative Spectroscopy and Radiative Transfer, 205, 127-134.

Sumlin, B. J., Heinson, Y. W., Shetty, N., Pandey, A., Pattison, R. S., Baker, S., . . . Chakrabarty, R. K. (2018b). UV–Vis–IR spectral complex refractive indices and optical properties of brown carbon aerosol from biomass burning. Journal of Quantitative Spectroscopy and Radiative Transfer, 206, 392-398.

Sun, H., Biedermann, L., & Bond, T. C. (2007). Color of brown carbon: A model for ultraviolet and visible light absorption by organic carbon aerosol. Geophysical Research Letters, 34(17).

Wang, X., Heald, C., Ridley, D., Schwarz, J., Spackman, J., Perring, A., . . . Clarke, A. (2014). Exploiting simultaneous observational constraints on mass and absorption to estimate the global direct radiative forcing of black carbon and brown carbon. Atmospheric Chemistry and Physics, 14(20), 10989-11010.

Wang, X., Heald, C. L., Liu, J., Weber, R. J., Campuzano-Jost, P., Jimenez, J. L., . . . Perring, A. E. (2018). Exploring the observational constraints on the simulation of brown carbon. Atmos. Chem. Phys., 18(2), 635-653. doi: 10.5194/acp-18-635-2018

Washenfelder, R., Attwood, A., Brock, C., Guo, H., Xu, L., Weber, R., . . . Baumann, K. (2015). Biomass burning dominates brown carbon absorption in the rural southeastern United States. Geophysical Research Letters, 42(2), 653-664.

Xie, M., Chen, X., Hays, M. D., & Holder, A. L. (2019). Composition and light absorption of N-containing aromatic compounds in organic aerosols from laboratory biomass burning. Atmospheric Chemistry and Physics, 19(5), 2899-2915.

Xie, M., Hays, M. D., & Holder, A. L. (2017). Light-absorbing organic carbon from prescribed and laboratory biomass burning and gasoline vehicle emissions. Scientific reports, 7(1), 7318.

Yang, M., Howell, S., Zhuang, J., & Huebert, B. (2009). Attribution of aerosol light absorption to black carbon, brown carbon, and dust in China–interpretations of atmospheric measurements during EAST-AIRE. Atmospheric Chemistry and Physics, 9(6), 2035-2050.

Zhang, X., Lin, Y. H., Surratt, J. D., & Weber, R. J. (2013). Sources, composition and absorption Ångstrom exponent of light-absorbing organic components in aerosol extracts from the Los Angeles Basin. Environmental science & technology, 47(8), 3685-3693.

Zhang, X., Wang, Y., Zhang, X., Guo, W., & Gong, S. (2008). Carbonaceous aerosol composition over various regions of China during 2006. Journal of Geophysical Research: Atmospheres, 113(D14).

Zhang, Y., Forrister, H., Liu, J., Dibb, J., Anderson, B., Schwarz, J. P., . . . Wang, Y. (2017). Top-of-atmosphere radiative forcing affected by brown carbon in the upper troposphere. Nature Geoscience, 10(7), 486.

Zhou, Y., Xing, X., Lang, J., Chen, D., Cheng, S., Lin, W., . . . Liu, C. (2017). A comprehensive biomass burning emission inventory with high spatial and temporal resolution in China. Atmospheric Chemistry and Physics, 17(4), 2839.

873 **Figures and Tables:**

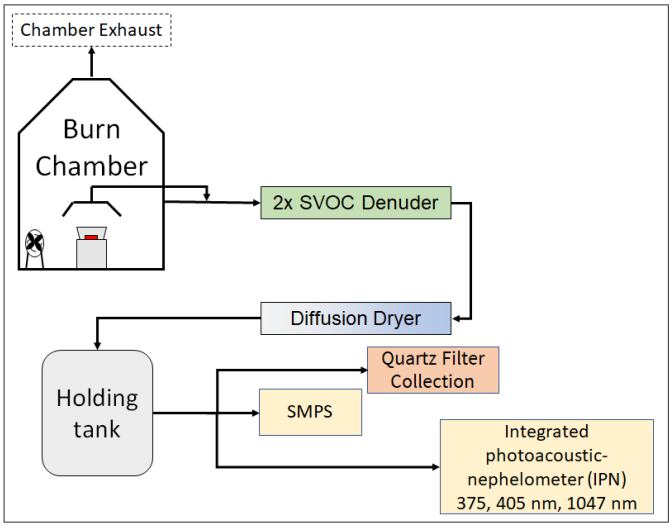

874

875 **Fig. 1:** A schematic representing the experimental setup. The aerosol emissions were either
876 sampled directly from the chamber wall or through a hood placed directly above the combusting
877 biomass.

878

879

880

881

882

883

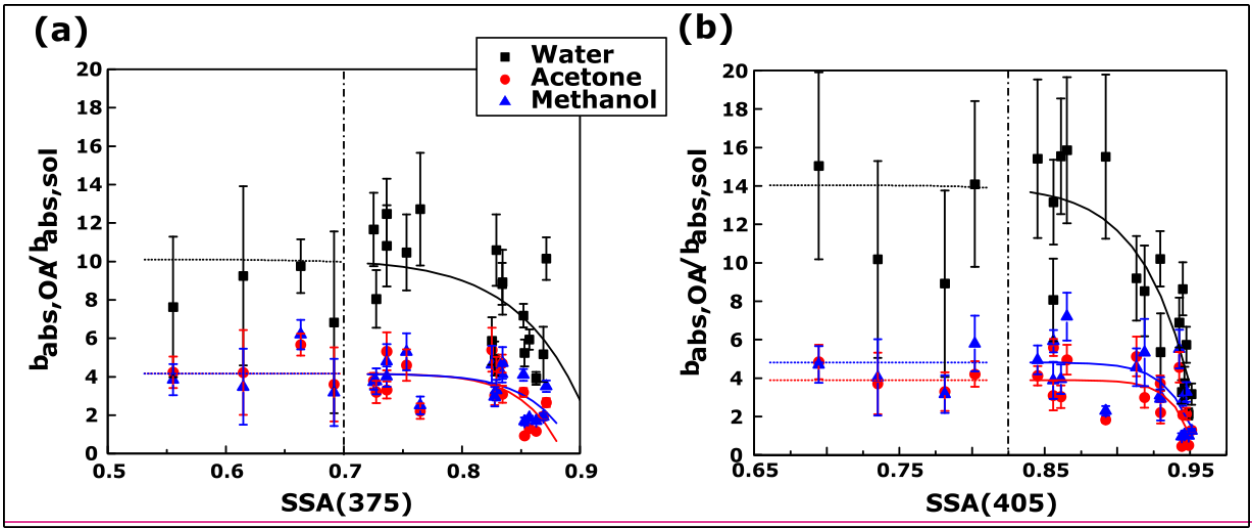

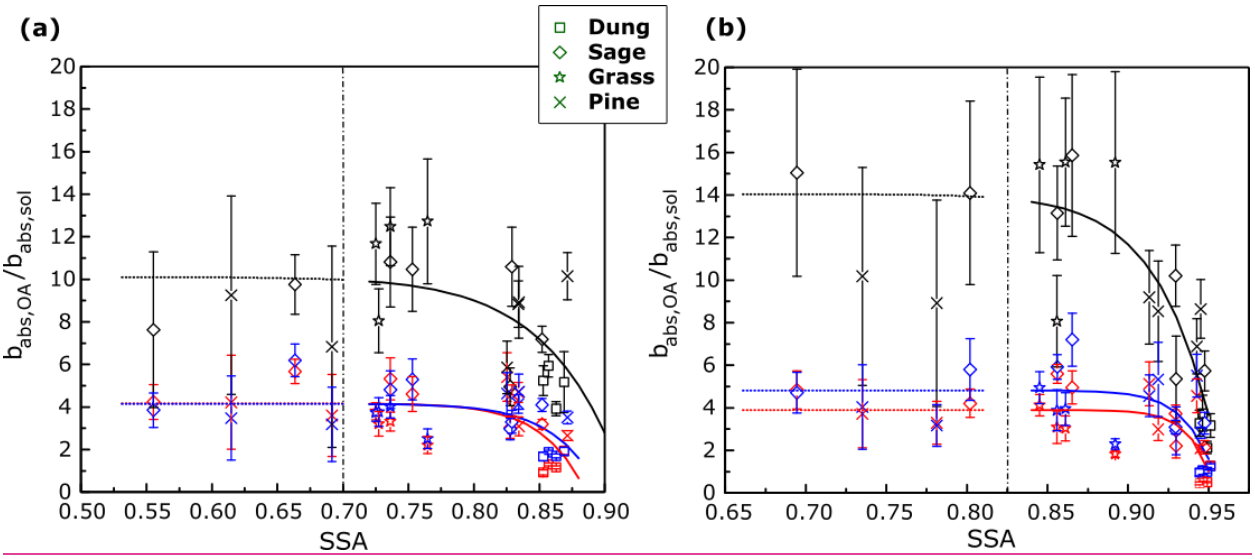

Fig. 2: Variation in $b_{abs,OA}/b_{abs,sol}$ ~~$b_{abs,OA}/b_{abs,sol}$~~ with change in the SSA at (a) 375 nm and (b) 405 nm (N = 21). The error bars represent one standard deviation from the mean and were calculated using Monte Carlo simulations. The black markers represent water extracts, red markers represent acetone extracts and blue markers represent methanol extracts. The perforated lines separate points at lower SSA, which have high errors greater than 30% due to uncertainties in BC $AÅE$ ~~AÅE~~, from the data at high SSA.

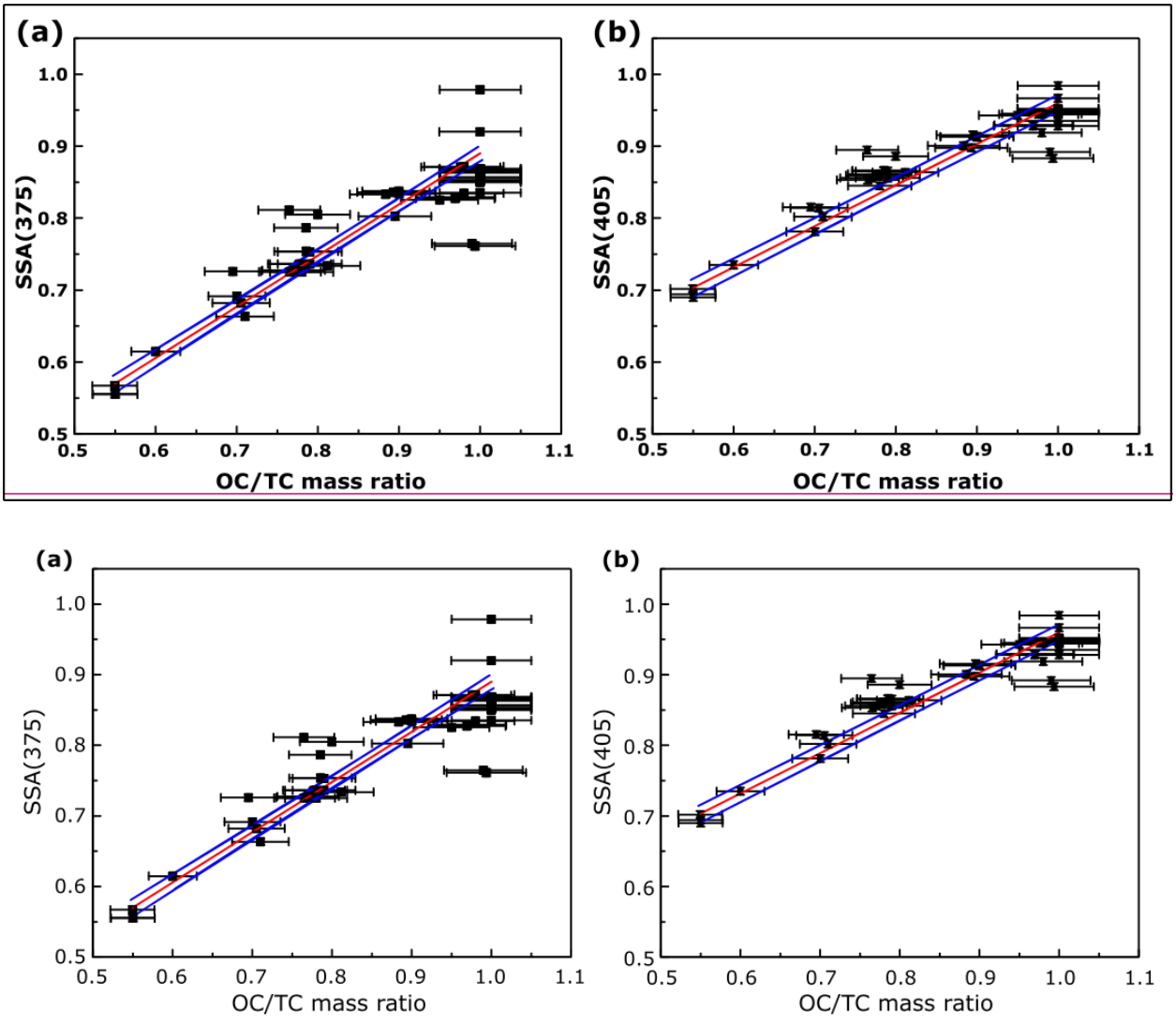

Fig. 3: SSA at (a) 375 nm and (b) 405 nm as a function of the OC/TC ratio (N= 49). The solid red lines are ODR fits to the data and the solid blue lines represent the 95% confidence intervals. The errors in OC/TC ratios were determined by the quadrature sum of uncertainties from EC/OC analysis and the error in SSA were negligible

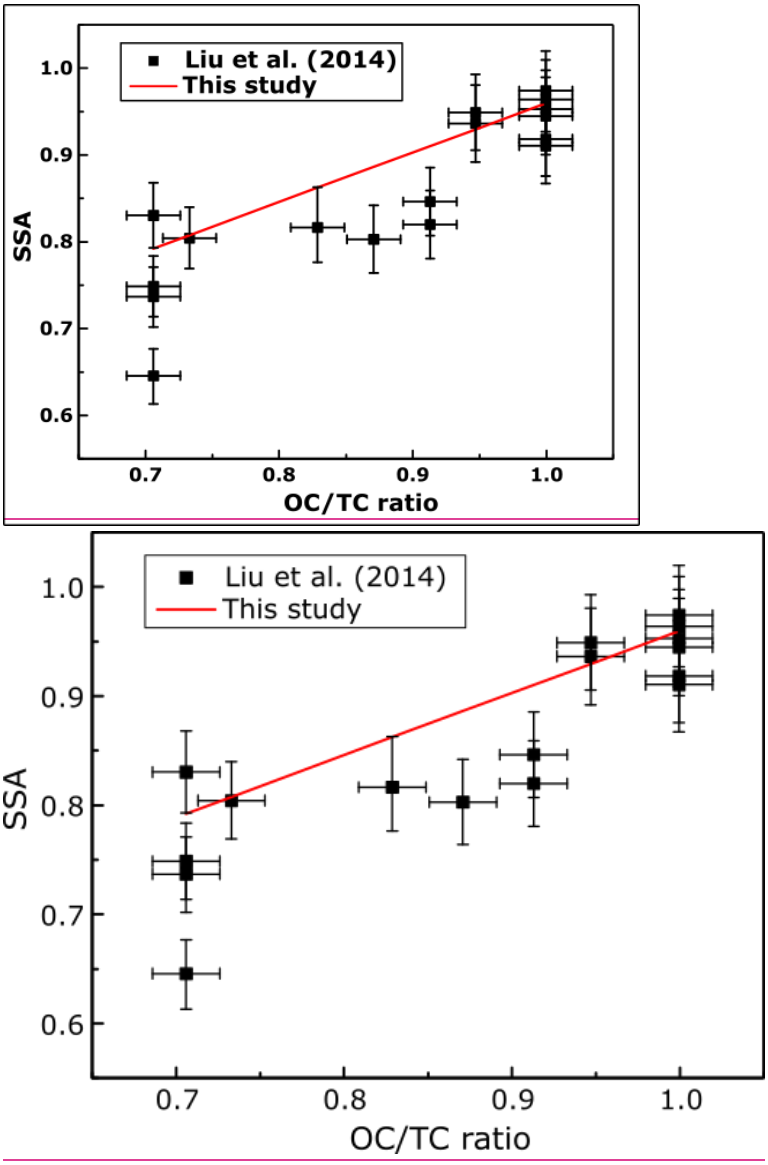

Fig. 4: Measured SSA values by Liu et al. (2014) for controlled laboratory combustion experiments plotted with the solid red line representing the ODR parametrization determined in this study.

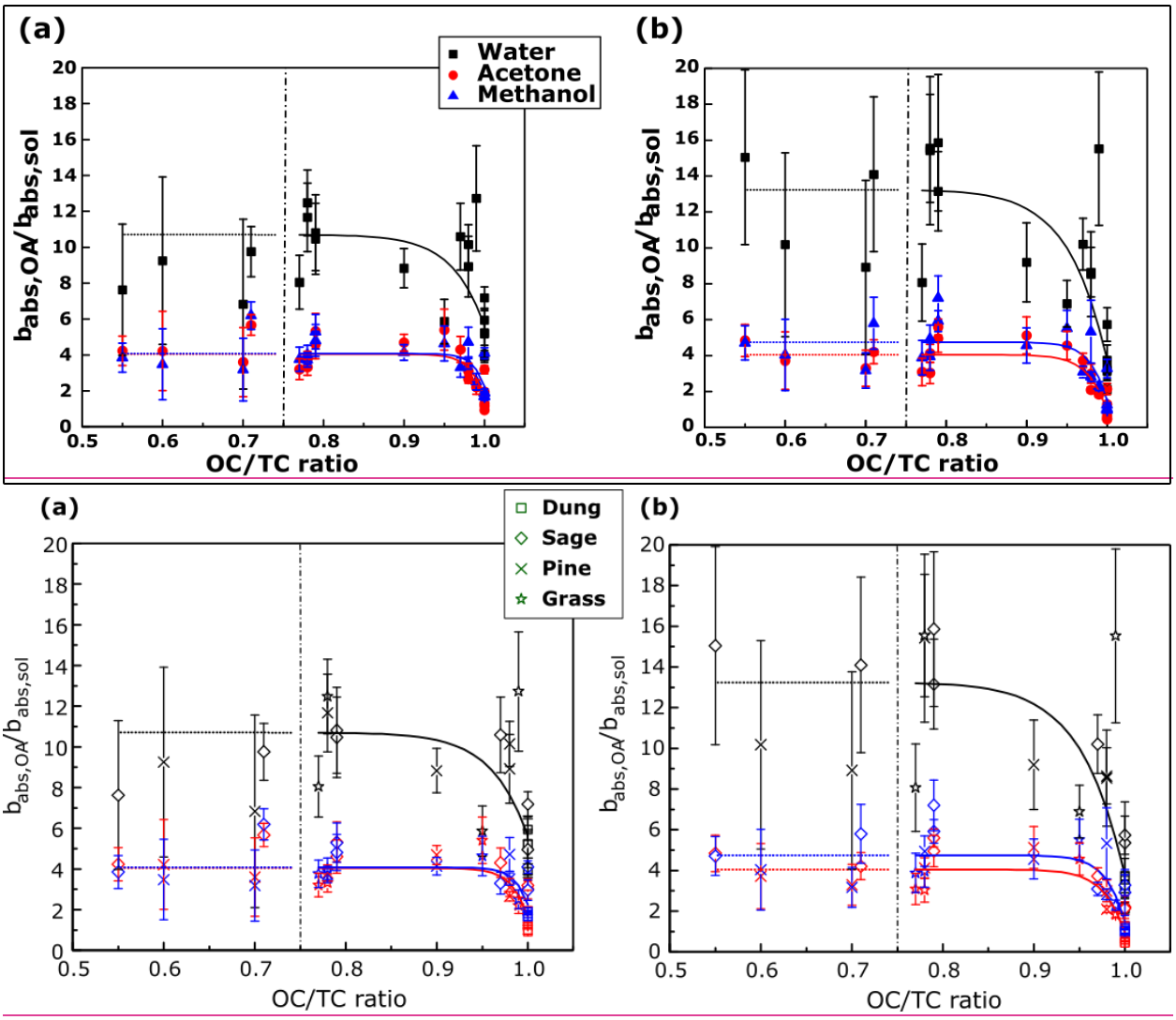

Fig. 5: The values of $b_{abs,OA}/b_{abs,sol}$ ~~$b_{abs,OA}/b_{abs,sol}$~~ plotted with the OC/TC ratio, instead of the SSA, as in Fig. 2. Black markers represent data for water extracts, red markers represent data for acetone extracts, and blue markers represent data for methanol extracts.

Table 1: Fit coefficients for $b_{abs,OA}/b_{abs,sol}$ ~~$b_{abs,OA}(\lambda)/b_{abs,sol}(\lambda)$~~ as a function of SSA ($y = k0 + k1\ (SSA)^{k_2}$) for tested solvents and the fuels analyzed in this study along with the RMSE value for each fit.

	Wavelength (nm)	Solvent	Fit Parameters			
			k_0	k_1	k_2	RMSE
$\frac{b_{abs,OA}}{b_{abs,sol}}$	375	Water	10.1 (±2.1)	-39.83 (±177.1)	16.109 (±31.3)	2.21
		Acetone	4.217 (±0.8)	-117.4 (±36.9)	27.546 (±37.5)	1.12
		Methanol	4.216 (±0.877)	-69.12 (±451.6)	25.876 (±45.4)	1.106
	405	Water	14.04 (±4.2)	-42.437 (±70.5)	27.42 (±35.5)	2.6
		Acetone	3.89 (±1.12)	-95.6 (±609.9)	68.3 (±121.8)	1.3
		Methanol	4.82 (±1.4)	-49.105 (±250.3)	53.107 (±98)	1.548

913 Table 2. ODR regression coefficients along with errors in brackets for plots of SSA v/s OC/TC
914 ratios (y = m (OC/TC) + c) for the different biomass fuels used in this study, and parameters for
915 ODR fit from Pokhrel et al. (2016) for 405 nm, along with RMSE values for our fits.

	Wavelength (nm)	m	c	RMSE
This study	375	0.71 (±0.04)	0.18 (±0.03)	0.04
	405	0.57 (± 0.02)	0.39 (± 0.02)	0.02
Pokhrel	405	1.07 (±0.04)	-0.13 (±0.04)	~~

916

Table 3: Fit parameters for ratios of the absorption coefficient of organics in the particle phase to the absorption coefficient of the solvent phase, as a function of the OC/TC ratio ($y = k_0 + k_1(OC/TC)^{k_2}$) for the fuels analyzed in this study, along with the RMSE value for each fit.

	Wavelength (nm)	Solvent	Fit Parameters			
			k_0	k_1	k_2	RMSE
$\frac{b_{abs,OA}}{b_{abs,bulk}}$	375	Water	10.7 (±1.83)	-5.105 (±2.54)	254.96 (±36.2)	2.0.01
		Acetone	4.105 (±0.877)	-2.437 (±1.21)	57.98 (±86.21)	1.00.98
		Methanol	4.108 (±0.7)	-1.82 (±1.11)	71.54 (±139.6)	0.9
	405	Water	13.24 (±2.41)	-9.546 (±3.215)	20.81 (±20.94)	2.547
		Acetone	4.105 (±0.985)	-3.108 (±1.329)	43.329 (±49.62)	1.0.04
		Methanol	4.875 (±1.107)	-3.24 (±1.765)	49.02 (±69.546)	1.33

Table 4: The ~~AÅE~~ $AÅE$ of OA from various fuels extracted in water, acetone, and methanol, along with the $AÅE$ ~~AÅE~~ calculated for $b_{abs,OA}$ ~~$b_{abs,OA}$~~.

Fuel	OC/TC ratio	$AÅE_{375-405}$ ~~AÅE$_{375-405}$~~			
		OA	Water	Acetone	Methanol
Dung	1	13.74 ± 2.327	8.0.00 ± 2.0.02	5.329 ± 1.43	5.21 ± 1.329
	1	15.32 ± 2.364	8.9.05 ± 2.0.04	5.985 ± 0.44	7.875 ± 0.64
	1	15.567 ± 0.657	7.548 ± 1.84	4.62 ± 0.31	4.5 ± 0.91
	1	14.93 ± 2.73	8.655 ± 1.219	5.325 ± 0.2	6.8 ± 0.439
Sage	1	13.93 ± 1.91	10.987 ± 1.219	8.62 ± 0.769	8.8 ± 1.12
	1	10.765 ± 1.547	10.71 ± 4.54	6.329 ± 3.2	7.3 ± 2.9
	0.97	10.658 ± 2.41	9.988 ± 1.42	5.2 ± 0.879	5.8 ± 0.769
	0.79	7.436 ± 2.988	12.328 ± 2.4	8.62 ± 0.876	9.217 ± 1.2
	0.79	8.21 ± 2.40	10.658 ± 2.215	8.73 ± 0.83	8.3 ± 1.3
	0.71	10.436 ± 1.41	7.5 ± 3.11	6.329 ± 1.71	6.4 ± 2.11
	0.55	9.94 ± 4.21	6.548 ± 4.877	3.84 ± 2.01.97	3.6 ± 2.8
Grass	0.99	10.105 ± 2.43	12.108 ± 4.56	7.84 ± 0.93	7.5 ± 1.23
	0.78	9.92 ± 3.11	10.215 ± 2.325	8.547 ± 0.547	9.6 ± 0.62
	0.78	6.987 ± 1.73	9.7 ± 3.875	7.549 ± 0.81	7.3 ± 1.6
	0.77	8.99.0 ± 4.0.04	8.21 ± 1.658	8.12 ± 0.62	8.4 ± 0.92
Pine	0.98	11.82 ± 1.0.04	9.436 ± 2.0	8.655 ± 0.875	8.1 ± 1.108
	0.98	8.768 ± 1.89	9.659 ± 3.439	8.436 ± 1.83	8.6 ± 1.53
	0.95	14.20 ± 3.53	16.44 ± 1.34	11.81 ± 0.91	12.8 ± 1.327
	0.9	8.24 ± 2.436	9.109 ± 2.33	8.875 ± 1.63	8.7 ± 2.01.97
	0.7	165.96 ± 10.987	9.93 ± 3.13	6.33 ± 2.24	5.83 ± 2.108
	0.6	17.41 ± 10.81	6.436 ± 3.31	5.2 ± 2.81	5.4 ± 2.91

Table 5: Correction factors for bulk solution absorption to particle phase absorption, based on Mie Theory calculations.

Fuel	Geometric mean (in nm)	Geometric standard deviation	Mie based Scaling Factor 375 nm	Mie based Scaling Factor 405 nm	IPN based bias 375 nm	IPN based bias 405 nm
Sage	397	1.3	2.0.04 ± 0.438	2.327 ± 0.41	2.6 ± 0.61	1.64 ± 0.655
	271	1.32	2.105 ± 0.438	2.329 ± 0.41	2.8 ± 0.657	1.987 ± 0.32
	159	1.59	2.01.99 ± 0.364	2.215 ± 0.439	2.81 ± 0.52	1.83 ± 0.437